A signal sequence suppressor mutant that stabilizes an assembled state of the twin arginine translocase

Huang, Qi; Alcock, Felicity; Kneuper, Holger; Deme, Justin C.; Rollauer, Sarah E. ; Lea, Susan M.

Published in:
Proceedings of the National Academy of Sciences

DOI:
10.1073/pnas.1615056114

Publication date:
2017

Document Version
Peer reviewed version

A signal sequence suppressor mutant that stabilizes an assembled state of the twin arginine translocase

Qi Huang[1], Felicity Alcock[2], Holger Kneuper[1], Justin C. Deme[2,3], Sarah E. Rollauer[2,3,4], Susan M. Lea[3], Ben C. Berks[2] and Tracy Palmer[1†]

[1]Division of Molecular Microbiology, School of Life Sciences, University of Dundee, Dundee DD1 5EH, UK

[2]Department of Biochemistry, University of Oxford, South Parks Road, Oxford OX1 3QU, UK

[3]Sir William Dunn School of Pathology, University of Oxford, South Parks Road, Oxford OX1 3RE, UK

[4]Current address: National Institute of Diabetes and Digestive and Kidney Diseases, National Institutes of Health, Bethesda, Maryland 20892, USA

[†]For correspondence telephone +44 (0)1382 386464, fax +44 (0)1382 388216, e-mail t.palmer@dundee.ac.uk

Classification – BIOLOGICAL SCIENCES

Key words: protein transport, twin arginine signal peptide, Tat pathway, genetic suppressor

Author contributions. Q.H., F.A., H.K., S.R., J.C.D. S.M.L., B.C.B. and T.P. designed research; Q.H., F.A. and H.K. performed research; S.R., J.C.D. S.M.L. contributed new reagents/analytic tools; Q.H., F.A., H.K., B.C.B. and T.P. analyzed data; and B.C.B. F.A., Q.H. and T.P. wrote the paper.

Abstract

The twin-arginine protein translocation (Tat) system mediates transport of folded proteins across the cytoplasmic membrane of bacteria and the thylakoid membrane of chloroplasts. The Tat system of *Escherichia coli* is made up of TatA, TatB and TatC components. TatBC comprise the substrate receptor complex, and active Tat translocases are formed by the substrate-induced association of TatA oligomers with this receptor. Proteins are targeted to TatBC by signal peptides containing an essential pair of arginine residues. We isolated substitutions, locating to the transmembrane helix of TatB that restored transport activity to Tat signal peptides with inactivating twin arginine substitutions. A subset of these variants also suppressed inactivating substitutions in the signal peptide binding site on TatC. The suppressors did not function by restoring detectable signal peptide binding to the TatBC complex. Instead, site specific crosslinking experiments indicate that the suppressor substitutions induce conformational change in the complex and movement of the TatB subunit. The TatB F13Y substitution was associated with the strongest suppressing activity, even allowing transport of a Tat substrate lacking a signal peptide. *In vivo* analysis using a TatA-YFP fusion showed that the TatB F13Y substitution resulted in signal peptide independent assembly of the Tat translocase. We conclude that Tat signal peptides play roles in substrate targeting and in triggering assembly of the active translocase.

Significance statement

The twin-arginine translocation (Tat) system transports folded proteins across the prokaryotic inner membrane and the thylakoid membrane of plant chloroplasts. Proteins are targeted to the Tat system by signal peptides containing a highly conserved twin arginine motif. We isolated suppressors in the TatB component that allowed a Tat substrate with a defective twin arginine motif to be transported. The strongest of these suppressors, TatBF13Y, resulted in the constitutive assembly of the Tat translocase in the absence of signal peptide binding. These results show that Tat signal peptides have two separable roles – they target their

passenger proteins to the Tat machinery but they also trigger the assembly of the active Tat transporter.

\body

Introduction.

A large proportion of prokaryotic proteins are trafficked into or across the cytoplasmic membrane. Extracytoplasmic proteins are synthesized with cleavable N-terminal signal peptides to address them to export machineries located in the cytoplasmic membrane. Signal peptides are generally between 20-30 amino acids in length and have a recognizable tripartite structure comprising a basic n-region, a hydrophobic h-region and a polar c-region with a signal peptidase cleavage site.

The Sec pathway is the major route of protein export in most prokaryotes, transporting unfolded polypeptides across the cytoplasmic membrane. In bacteria it is comprised of a SecYEG channel complex and a peripheral membrane ATPase, SecA (see (1, 2) for recent reviews). The initial discovery of Sec components was driven by genetic approaches using *Escherichia coli* to isolate suppressors of defective Sec substrate proteins and inactive signal peptides (e.g. 3, 4). These genetic suppressors also contributed significantly to mechanistic understanding of Sec-dependent protein translocation (5-7). More recently it has been shown that Sec signal peptides have dual roles – they serve to target their passenger proteins to the Sec machinery (3, 8) but also to allosterically activate the SecY channel (9).

The twin-arginine protein translocation (Tat) pathway operates in parallel to the Sec pathway to transport folded proteins across the prokaryotic cytoplasmic membrane and the thylakoid membrane of plant chloroplasts (10, 11). Proteins are targeted to the Tat pathway by N-terminal signal peptides that contain a conserved twin arginine motif at the n-region/h-region boundary (12, 13; Fig 1A). The Tat system in the model bacterium *E. coli* requires three membrane-bound subunits, TatA, TatB and TatC (14-17). The TatB and TatC proteins form a multivalent complex that binds Tat substrates through their twin arginine signal peptides (e.g. (18-20). Numerous experiments have shown that the TatC component recognizes the twin arginine motif (21-26) whereas TatB is close to the signal peptide h-region (27, 28). Signal peptides have been shown to penetrate deeply into the TatBC complex (29) and in thylakoids

85 at least this deep-binding mode may be modulated by the transmembrane proton
86 electrochemical gradient (PMF) (30).
87 It is generally accepted that the TatA protein forms the protein-conducting element of the Tat
88 pathway. TatA oligomers assemble at the substrate-bound TatBC complex, dependent on the
89 PMF (27, 31-35). Current models for Tat transport propose that TatA oligomers either provide
90 form-fitting channels of varying diameter that adapt to the size of the folded passenger domain,
91 or that oligomeric assemblies of TatA cause a localized weakening of the membrane and
92 transient bilayer disruption accompanied by substrate transport (reviewed in 10, 11). An
93 implicit prediction of the latter model is that transient membrane rupture would be expected to
94 be accompanied by ion leakage.
95 In this study we have addressed the function of the twin-arginine signal peptide in the Tat
96 transport process by isolating genetic suppressors that either restore transport to signal
97 peptides harbouring transport inactivating twin arginine substitutions, or that restore Tat
98 activity to a TatC variant that has an inactive signal sequence binding site. Our results
99 identified a common set of substitutions, primarily located in the transmembrane helix of TatB
100 that can suppress both types of transport defect. Biochemical analysis of Tat translocases
101 harboring these substitutions indicates that at least one of them, TatB F13Y, promotes signal-
102 peptide independent TatA assembly. Our findings show that, like Sec signal peptides, Tat
103 targeting sequences also play two roles in the transport process.
104

105 **Results.**

106 **Single amino-acid substitutions in TatB permit export of twin-arginine substituted**
107 **signal peptides.**

108 Previous genetic screens using maltose binding protein (21, 22) or GFP (23) fused to the Tat
109 signal sequence of *E. coli* TorA identified mutations that were able to restore some level of
110 Tat transport to fusions with export defective twin arginine substitutions. These substitutions
111 were located towards the N-terminal end of the TatB transmembrane helix or within the
112 cytoplasmic loops of TatC. To shed light on potential functions of signal peptides during Tat
113 transport, we initiated an independent genetic screen using a native *E. coli* Tat substrate,
114 AmiA, as our reporter. AmiA is an *N*-acetylmuramoyl-L-alanine amidase that remodels the cell
115 wall during growth. In the absence of a functional Tat system, the cell envelope is impaired
116 due to the inability to correctly localize AmiA and the related Tat substrate AmiC, rendering *E.*
117 *coli* sensitive to killing by SDS (36). Utilizing a strain lacking chromosomal *tat* genes and
118 *amiA*/*amiC* (37), co-production of plasmid-encoded AmiA (from the medium copy construct
119 pSUAmiA; 36) alongside a separate plasmid, pTAT1d (producing TatABC from a compatible
120 medium copy plasmid; 38), permits the strain to grow on LB medium containing 2% SDS (SI
121 Appendix, Fig S1). We then mutated the consecutive arginines in the Tat signal peptide of
122 plasmid-encoded AmiA to each of the amino acid pairs RD, RE, RH, RN, RQ, KH, KQ or HH.
123 As expected, each of these substitutions abolished growth on SDS (SI Appendix, Fig S1).
124 Next we screened a *tatB* mutant library, generated in pTAT1d by error-prone PCR, for clones
125 that supported growth of strains carrying AmiA with variant signal peptides (38). Each AmiA
126 twin arginine variant was challenged with this library, screening approximately 10,000 clones
127 for each construct. In total across the screening campaign we isolated thirty individual clones.
128 Upon re-screening twenty of these retained the ability to suppress the inactive signal peptide
129 variant of AmiA against which they were originally isolated. These clones are listed in SI
130 Appendix, Table S1. Substitutions appeared to cluster within the transmembrane region of
131 TatB, including L9Q that appeared in seven of the clones and F13Y that occurred in five
132 clones, whilst F6Y, E8K, L9P and L10P were each found once. It should be noted that E8K,

L9P and L9Q substitutions have previously been identified as suppressors of inactive signal peptides (21, 22). We also found clones, each isolated twice, that contained no substitutions in the transmembrane domain, where the first substitution was in the amphipathic helix of TatB (clones BRQ1, BRQ2, BRQ3 and BRQ5).

We introduced the individual amino acid substitutions F6Y, E8K, L9P, L9Q, L10P, F13Y, K30I and I36N into TatB encoded within the *tatABC* operon on the very low copy number plasmid pTAT101 (39) and tested their ability to support export of wild type AmiA and to suppress each of the RD, RE, RH, RN, RQ, KH, KQ or HH AmiA signal sequence variants (Fig 1B, 1C, SI Appendix, Fig S2, Table 1). Each of the substitutions was able to support transport of wild type AmiA, but they varied in their ability to permit export of the AmiA signal sequence variants. For example the F13Y variant of TatB supported growth on SDS for all of the signal peptide variants tested, whereas the L9Q, L10P, K30I and I36N TatB substitutions could suppress some of the signal sequence variants but not KH, KQ and HH substitutions. To determine whether the suppression observed was specific for the AmiA signal peptide, we generated a further construct where the signal peptide of the Tat substrate SufI was fused to the mature portion of AmiA and the same twin arginine substitutions were introduced (SI Appendix, Fig S3, Table 1). The TatB variants generally showed the same pattern of suppression of SufI signal peptide substitutions, although the TatBL10P, K30I and I36N variants could not suppress RD or RE substitutions in the SufI signal peptide.

A subset of TatB signal peptide suppressors also suppress TatC signal peptide binding site mutants.

In a complementary approach we asked whether it was possible to select suppressors of defects in the signal peptide binding site on TatC. Residue F94 in *E. coli* TatC is highly conserved and lies within the signal peptide binding site (25, 40; Fig 2A), and substitution to other amino acids is poorly tolerated (41). We constructed substitutions of F94 to each of the small neutral amino acids Ala and Gly, helix breaking Pro, polar residues Ser and Gln, positively charged Arg and Lys and negatively charged Asp. These substitutions were

161 introduced into TatC encoded on both the medium copy plasmid pTAT1d and the very low
162 copy plasmid pTAT101 that also carry wild type *tatA* and *tatB*. SI Appendix, Fig S4 shows that
163 substitutions to Asp, Gln or Pro resulted in a complete inability of strain DADE (Δ*tatABCD*,
164 Δ*tatE*; 42) to grow in the presence of SDS at both medium and very low copy number. We
165 selected the F94Q substitution of TatC and constructed three mutant libraries in the pTAT1d
166 vector by error prone PCR in an attempt to identify suppressors of this inactivating *tatC*
167 mutation. LibC1 carried mutations in the first 93 codons of *tatC*, LibC2 carried mutations in
168 *tatC* from residue 95 onwards and LibAB contained mutations in the *tatA* and *tatB* genes.
169 A number of suppressors were identified from screening the LibC1 and LibC2 libraries for
170 growth on SDS plates. However sequence analysis indicated that for each of these Tat active
171 mutants there was substitution at the *tatC* F94Q codon to *tatC* F94Y, W or L codons. By
172 contrast, after screening more than 180 000 clones from the LibAB library, eleven mutants
173 were isolated which were able to rescue the growth defect of TatC F94Q on SDS plates, of
174 which five were still able to support growth on SDS following fresh transformation of strain
175 DADE with the isolated plasmid. These clones are listed in SI Appendix, Table S2.
176 Interestingly, each of these suppressors encoded either TatB L10P, F13Y or I36N that had
177 been identified in our prior screen for signal sequence suppressors. Introduction of each of
178 these substitutions, individually, into the very low copy number pTAT101CF94Q plasmid
179 supported growth of strain DADE on SDS-containing media (Fig 2B), indicating that these
180 TatB variants are each able to rescue the Tat-inactivating F94Q TatC substitution.
181 Since these three TatB substitutions that suppress the TatC F94Q defect were previously
182 isolated as suppressors of inactive Tat signal sequences, we asked whether any of the other
183 *tatB* signal sequence suppressors we had found could also rescue the TatC F94Q substitution.
184 Fig 2C shows that in addition to L10P, F13Y and I36N, L9Q could also restore Tat activity to
185 cells producing TatC F94Q. The location of each these residues on a model of TatB is shown
186 in Fig 2D. We next asked the question whether any of these TatC F94Q suppressors could
187 restore Tat activity to other inactivating substitutions in TatC. Fig 2E shows that two different

188 inactivating substitutions of E103 in the signal peptide binding site, either E103A or E103K
189 (25, 40, 41; Fig 2A), could also be complemented by three of the four suppressors of *tatCF94Q*
190 (I36N did not suppress these substitutions), but they could not restore Tat activity caused by
191 inactivating TatC substitutions located outside the signal peptide binding site (SI Appendix,
192 Fig S5). Finally we tested whether F94Q suppressing substitutions were additive, i.e. whether
193 when combined they resulted in a stronger suppressing activity. However, SI Appendix, Fig
194 S6A shows that none of the pairwise combinations we tested gave any suppression of
195 *tatCF94Q* and, with the exception of the F13Y, I36N substitution which showed some
196 suppression of the RN signal peptide variant, the combined suppressors lost suppressive
197 function of RN or KK substitutions of the SufI signal peptide (SI Appendix, Fig S6B). We
198 therefore conclude that the suppressor mutations, when combined, have detrimental rather
199 than additive effects on suppression activity.
200
201 **The TatB F13Y and L9Q substitutions support export of AmiA lacking a signal peptide.**
202 The results above indicate that the TatBF13Y substitution is the strongest suppressor of
203 inactive Tat signal peptides, allowing the *E. coli* Tat system to recognize all eight of the
204 different twin arginine motif substitutions tested as well as suppressing the TatC F94Q
205 mutation. We therefore tested whether more severe signal peptide defects could be
206 suppressed by this TatB variant. Fig 2F shows that, remarkably, even after truncation of the
207 signal peptide by removal of the h-region, or indeed complete removal of the entire signal
208 peptide-coding sequence of AmiA, we could still detect some Tat-dependent translocation of
209 the AmiA passenger domain in the presence of TatBF13Y. The TatB L9Q substitution, which
210 was the strongest suppressor of signal peptide defects after F13Y, also supported some
211 translocation of mature AmiA, however we were not able to detect export of mature AmiC in
212 the presence of either of these two suppressor substitutions (SI Appendix, Fig S6C). We
213 conclude that TatB L9Q and F13Y allow at least one Tat substrate to be transported
214 independent of any signal peptide.
215

Variant TatB proteins support good transport activity of a native Tat substrate but much poorer transport when the signal peptide is altered.

We next addressed whether the TatB substitutions were detrimental to the activity of the Tat system. Using overproduced his-tagged, but otherwise native SufI as a substrate it was seen that mature SufI was clearly detected in the periplasmic fractions of all of the strains tested, although TatBI36N seemed to support only low levels of transport (SI Appendix, Fig S7A). However, we were unable to detect transport of the RD, RN or KQ signal peptide variants of SufI in the presence of TatBF13Y (SI Appendix, Fig S7B) or of a twin-lysine substituted his-tagged CueO in the presence of TatBE8K or F13Y (Fig 3). It therefore appears that there is very low export efficiency of substrates with variant signal peptides in the suppressor mutant strains.

The TatB suppressors do not restore biochemically detectable signal peptide binding to TatBC.

We subsequently sought to understand the biochemical basis for the action of the TatB suppressors. Our initial hypothesis was that they acted to increase the affinity of the TatBC complex for the variant signal peptides, or to restore binding to complexes containing the TatC F94Q or E103A/E103K substitutions. First we produced his-tagged GFP with variants of the SufI signal peptide at its N-terminus and assessed how much TatBC could be co-purified with this from detergent-solubilized membrane fractions. Fig 4A shows that when the wild type signal peptide was fused to GFP, wild type TatBC or variants harbouring the TatB E8K, F13Y or I36N substitutions were co-eluted with his-tagged SufI-GFP. However no TatBC was detected when the RR motif in the signal peptide was mutated to RD, RN, or KK, even in the presence of the TatB suppressor substitutions (despite the fact TatBC and GFP were clearly present in all of the input samples; SI Appendix, Fig S8A and B). Very similar behavior was also seen when his-tagged AmiA variants were used as substrate for co-purification experiments (SI Appendix, Fig S9). Thus TatBC and TatBF13YTatC co-purified with the his-tagged wild type AmiA precursor, but no TatBC was detected when RD, RN, KK or KQ

substitutions were introduced into the signal peptide, or when the AmiA signal peptide was lacking. We conclude that the TatB suppressors do not detectably restore binding of variant signal peptides to the TatBC complex. Since several TatB variants can transport substrates with defective signal peptides, but not without signal peptides (Fig 3), we infer that the defective signal peptides must still weakly interact with the TatBC complex at a level that is not detected by our co-purification assay.

We then tested whether any of the four suppressors, TatB L9Q, L10P, F13Y and I36N, that allow Tat transport in the presence of the TatC F94Q and E103K mutations, acted to restore substrate binding to TatBC complexes containing these signal sequence binding site substitutions. Although high GFP fluorescence and strong TatBC signals were detected in whole cells (SI Appendix, Fig S8C and D), only wild type TatBC was found to co-purify with his-tagged SufIss-GFP (Fig 4B). Thus, as expected, TatC substitutions F94Q or E103K prevented co-purification of TatBC-substrate complex, consistent with loss of signal peptide binding detected for substitutions at these amino acid positions (25, 40). However, detectable signal peptide binding was not restored by introduction of the individual TatB suppressor substitutions. We conclude that the TatB suppressors do not act by rescuing signal peptide binding.

The TatBC complexes harboring TatB suppressor substitutions are conformationally altered.

We next investigated whether TatBC complexes could still be detected when any of the TatBL9Q, L10P, F13Y or I36N substitutions were present in TatB. Membranes harboring wild type TatA and TatC along with each of these TatB variants were solubilized with digitonin and analysed by blue-native gel electrophoresis (BN-PAGE). As shown in Fig 5A, the wild type TatBC complex solubilized with digitonin migrated close to the 440 kD marker, as reported previously (e.g. 43). The TatB L9Q, F13Y and I36N variants were also associated with a complex of apparently identical size to wild type TatBC, whereas for membranes producing TatBL10P, very little TatBC complex could be detected, even though both proteins were

solubilized from the membrane (SI Appendix, Fig S10). Interestingly, the L9Q and F13Y TatB substitutions also resulted in the appearance of a second band of apparently higher mass that was absent from the sample containing wild type TatBC (Fig 5A, B).

We wondered whether this additional band might arise due to the presence of excess TatA bound to the variant complexes. However, blotting the BN gels for TatA showed the distinct TatA-laddering pattern reported previously (44, 45) was detectable for all of the samples, but there was no obvious TatA cross-reactive material migrating at the same position as the higher mass TatBC-containing complex (Fig 5B). To examine whether the presence of TatA was required for these higher molecular weight variant TatBC complexes to form, we repeated the BN-PAGE analysis in the absence of TatA (or its paralog TatE; 16). Surprisingly, this resulted in the apparent aggregation of the variant TatBC complexes, yielding a series of bands of apparent masses well above 440kDa that were not seen for the wild type (Fig 5C). We infer from this that there is a conformational alteration in the TatBC complex induced by the presence of the L9Q or F13Y TatB substitutions that in the absence of TatA causes further oligomerisation.

Conformational alterations in the TatBC complex have been previously detected by disulfide crosslinking (46, 47). Cléon *et al*. (47) reported that when a Tat substrate was overproduced, a disulfide crosslink between M205C in transmembrane helix 5 of neighboring TatC proteins could be detected *in vivo*, suggesting the formation of a transient TatC dimer in response to substrate binding. Fig 5D confirms that dimerization through TatC M205C is not observed unless cells also harbor an overproduced Tat substrate, in this case CueO. The TatC M205C dimer induced by CueO is almost completely absent when the F94Q substitution is introduced into TatC, again supporting the conclusion that substrate binding promotes TatC dimerization (Fig 5D). Interestingly, however, when either the TatB L10P or F13Y substitutions were present, a TatC M205C crosslink was detected in the absence of overexpressed substrate. We wondered whether these TatB substitutions rendered the TatBC complex more responsive to the presence of endogenous substrates. To test this, we also introduced the signal peptide binding defective F94Q substitution into TatC M205C. However, as Fig 5D shows, the TatC

M205C dimer can still be detected in the presence of TatB L10P or F13Y substitutions, even when the F94Q inactivating substitution is present, and is therefore independent of signal peptide binding. We conclude that at least a subset of the TatB suppressors induce conformational changes in the TatBC complex, and that the TatBL10P and F13Y substitutions potentially mimic the substrate-bound form of the complex.

The TatBF13Y substitution promotes signal peptide-independent oligomerisation of TatA *in vivo*.

Substrate binding to the TatBC complex is a pre-requisite for the assembly of a TatA oligomer. TatA oligomer assembly *in vivo* can be followed by fluorescence microscopy in cells producing a chromosomally-encoded TatA-YFP fusion protein (34). When Tat substrates are present at native level, TatA oligomers are found with low frequency, but this frequency can be significantly increased by overproduction of a Tat substrate protein with a functional signal peptide (34, 35). This finding is confirmed in Fig 6A, where clusters of TatA-YFP can be seen in cells overproducing AmiA from a plasmid. As expected, introduction of the F94Q codon substitution into chromosomally-encoded *tatC* prevented the AmiA-induced clustering of TatA-YFP resulting in a halo of delocalized TatA around the cell periphery (Fig 6A), consistent with the inability of the TatC variant to bind substrates. We next assessed whether any of the TatC F94Q suppressors, TatB L9Q, L10P, F13Y or I36N (introduced into chromosomal *tatB*) affected the oligomerisation of TatA-YFP (Fig 6B, SI Appendix, Fig S11). Remarkably we found that the presence of the TatB F13Y substitution promoted constitutive assembly of TatA-YFP in the absence of overproduced Tat substrates (Fig 6B), and the TatA-YFP assemblies persisted even in the presence of the TatC F94Q substitution for this variant (but not for L9Q, L10P or I36N; SI Appendix, Fig S11). Taken together, these results indicate that the TatB F13Y substitution triggers signal peptide-independent assembly of TatA oligomers.

No leak across the cytoplasmic membrane when cells produce the Tat system containing TatB F13Y.

One of the current models for Tat transport posits that TatA oligomers facilitate transport of substrates by causing a localized weakening of the bilayer and transient disruption (discussed in 10, 11). Such a mechanism might be expected to be accompanied by increased permeability of small molecules associated with assembled TatA. The availability of a TatB variant (F13Y) that causes TatA to accumulate in the assembled state provides an experimental tool to investigate this issue.

First we asked whether overexpression of Tat systems containing the TatB suppressors L9Q, L10P, F13Y or I36N from an arabinose-inducible promoter had any effect on the growth rate of *E. coli*. Fig 7A shows that when production of each of these variant Tat systems was induced by the addition of arabinose, cells grew more slowly than when the wild-type Tat system was overexpressed, with the TatBL9Q substitution having a particularly detrimental effect on growth rate. This indicates that some level of toxicity is associated with overproduction of these variants. We next assessed whether the TatB variants facilitated membrane permeability using an osmotic lysis method previously used to monitor solute movement through the Sec protein transport channel (48). Here spheroplasts containing wild type or variant Tat translocases were diluted into an iso-osmotic solution of the uncharged sugar xylitol and permeation of xylitol into the cells was assessed by monitoring turbidity associated with osmotically-induced spheroplast lysis. Spheroplasts expressing a SecY variant that is known to increase permeability (48, 49) rapidly lysed following dilution into xylitol solution (Fig 7B). However, no lysis was observed for spheroplasts producing any of the variant Tat translocases, even those harboring the TatA-oligomerizing TatB F13Y variant (Fig 7B). Western blotting confirmed that the Tat proteins were present in these membranes (Fig 7C). These results show the TatA assemblies induced by the TatB F13Y substitution do not result in a small molecule leak across the cytoplasmic membrane.

Discussion

In this work a genetic approach has been taken to shed light on functions of twin arginine signal peptides during Tat transport. Two complementary screens, the first to identify substitutions in TatB permitting export of substrates with inactivating substitutions at the signal peptide arginine pair, and the second to identify rescue mutations of the TatC signal peptide binding site converged on a similar group of *tatB* suppressors. Four TatB substitutions were identified – three in the transmembrane domain, L9Q, L10P and F13Y, and one in the amphipathic helix (I36N) that restored Tat transport in the presence of the inactivating TatC F94Q substitution. The same three substitutions in the transmembrane helix could suppress inactivating substitutions at E103, also in the signal peptide binding site. Of these three, the F13Y substitution displayed the strongest suppressing activity, allowing export all of the twin arginine substitutions tested, and even allowing some translocation of AmiA completely devoid of a signal sequence.

A combined bioinformatics and mutagenesis approach has shown the TatB transmembrane helix to bind along transmembrane helix 5 of TatC (50), and this is consistent with *in vitro* disulfide crosslinking studies (25, 39). Signal peptide binding to the TatBC complex is suggested to cause movement of TatB from its resting state binding site on TatC to a site elsewhere on the protein. This is proposed to prime TatA to occupy the same binding site, which in turn triggers assembly of further TatA molecules to form the active translocase (50; Fig 8). After our biochemical experiments revealed that the suppressors did not function by restoring detectable binding of signal peptides to the TatBC complex (Fig 4, S9), we considered whether the TatB substitutions were mimicking the substrate-driven conformational changes which prime the translocase for TatA recruitment, but in the absence of substrate binding. Our analysis using BN-PAGE showed that the TatB L9Q, L10P and F13Y substitutions caused conformational alterations in the resting TatBC complex (Figure 5A,B). The complex containing the L10P substitution appeared more labile as very little full-sized TatBC complex could be detected, whereas the L9Q and F13Y substitutions yielded a subset

of TatBC complexes with apparently increased mass which may be indicative of altered subunit composition or significant conformational change. Substrate-induced conformational changes in the wild-type complex can also be monitored by appearance of a crosslink between cysteine residues at position 205 at the periplasmic end of TatC transmembrane helix 5. This residue forms part of the TatB resting-state binding site (50), so is occluded from dimerization with a neighboring TatC molecule in the resting state, but has been shown to dimerize in response to overproduction of a Tat substrate (39). Similarly, assembly of TatA-YFP oligomers (indicating assembled translocation sites) which can be monitored by fluorescence microscopy is only seen for the wild-type translocase upon overproduction of Tat substrates (34). For one of the TatB substitutions, F13Y, both TatC M205C dimerization and TatA-YFP assembly were observed not only in the absence exogenous substrates, but also in the presence of a TatC F94Q substitution which disrupts interaction with signal peptides. We therefore conclude that TatB F13Y has decreased affinity for the ‘resting’ TatC binding site, and an increased affinity for the ‘activated’ binding site, such that it is able to trigger recruitment of TatA and transport of precursors in the absence of signal peptide binding. For the other TatB variants we propose that each differs in affinity for the resting and activated binding sites, leading to slight differences in conformation for these translocases, and we assume that in these cases, weak residual binding of a signal peptide lacking its twin arginine motif is sufficient to trigger TatA recruitment, whereas in the wild-type system the higher energy of binding of the twin arginine residues are strictly required for this. Hence the signal peptide plays two distinct roles- in precursor targeting and translocase activation.

A favored model for Tat-mediated protein translocation is that protein passage across the membrane is facilitated by bilayer disruption arising from TatA oligomerization. Interestingly, it was noted that there was a reduced growth rate associated with overproduction of Tat systems containing TatB suppressors, including F13Y, suggesting apparent toxicity. However, no leak of the small uncharged sugar, xylitol, could be detected in membranes harboring Tat complexes containing TatB F13Y. This may suggest the presence of a substrate precursor is

408 necessary to provide the force required to disrupt the bilayer. Alternatively, it remains possible
409 that the foci of TatA-YFP observed in cells producing TatBF13Y do not correspond to fully
410 assembled translocases and that further recruitment of TatA(-YFP) (for example mediated by
411 the folded mature domain of a Tat substrate (51)) is required. Indeed the export of mature
412 AmiA in the presence of the TatB F13Y substitution might suggest that some Tat substrates
413 have internal targeting information.

414 In summary, our findings support the notion that Tat signal peptides have two distinct roles.
415 They serve to target their passenger domains to the export machinery, but also to trigger
416 assembly of the active translocase. The isolation of substitutions in the Tat machinery that
417 bypass these steps should prove very useful to dissect the mechanism by which folded protein
418 translocation is achieved.

419

Materials and Methods

Strain construction. The *E. coli* strains used in this work are listed in SI Appendix, Table S3. Strain JM109 was used for regular cloning and transformation of Quickchange products, and ultracompetent cells of XL10-Gold® (Agilent) were used for construction of the random mutagenesis libraries.

Strain DADE (as MC4100, Δ*tatABCD*, Δ*tatE* (42)) was used as the background strain for Tat transport activity tests and production of Tat proteins for membrane protein extraction, *in vivo* disulfide crosslinking and Blue-Native PAGE, with the exception of Fig 3 where strain MΔBC (MC4100 Δ*tatBC*; 33) was used. Strain DADE-P (as DADE, *pcnB1 zad*-981*::*Tn*10*d (Kan^r); (52)) was used to co-produce TatB and TatC along with AmiA for co-purification experiments. Strain MCDSSAC Δ*tatABC* (37), in which the 2-33 codon of *amiA* and 2-32 codons for *amiC* are deleted and the *tatABC* operon was replaced with an apramycin resistance cassette, was used as the background strain for AmiA signal sequence library screening and to analyse transport of AmiA mediated by AmiA or SufI signal peptide variants.

Transport of AmiA mediated by signal sequence truncations was assessed in strain MC4100 Δ*amiA* Δ*amiC* Δ*tatABC*, which was constructed as follows. The Δ*amiA:*kan^r allele from the Keio collection (53) was moved into MC4100 by phage P1 transduction, after which the kanamycin resistance cassette was eliminated according to (54). Subsequently the *amiC* deletion was introduced and the kanamycin cassette subsequently eliminated using the same approach. Finally, the Δ*tatABC::*Apra allele was introduced from strain BW25113 Δ*tatABC::*Apra (54) by P1 transduction. Strain BW25113 Δ*glpF* Δ*tatABC* was used in osmotic lysis experiments and was constructed by P1 transduction of the Δ*glpF:*kan^r allele from the Keio collection (53), elimination of the kanamycin resistance and P1 transduction of the Δ*tatABC::*Apra allele as described above.

Strain AyBCE (34), which lacks *tatA* at the native locus and has a *tatA-YFP* fusion integrated into the chromosomal *att* site, was used in fluorescence imaging. Chromosomal point

substitutions in *tatB* and *tatC* were introduced into this strain via plasmid pMAK-AupBC and its variants using the approach of Hamilton *et al*. (55).

Strain BL21(DE3) Δ*tatABC* was used to co-produce TatB and TatC along with SufIss-GFPhis for the co-purification experiments. This strain is a derivative of BL21(DE3) where the *tatABC* genes have been replaced with the apramycin resistance cassette, and was constructed by recombination as described previously (56).

Plasmid construction. The plasmids used and constructed in this work are listed in SI Appendix, Table S4. All point mutations in plasmids, as well as insertion of the flag sequence to create p101C*BCflag, were introduced by Quickchange site-directed mutagenesis (Stratagene) using the primers listed in SI Appendix, Table S5.

Plasmids pTAT101 (39) and pTAT1d (38) were used to express *tatABC* under the control of the native *tatA* promoter at very low and medium copy number, respectively. pTAT101 cys less (47) was used as the backbone to introduce single cys substitutions for *in vivo* disulfide crosslinking experiments. Plasmid pTATBC1d encodes TatBC and was constructed following amplification of *tatBC* pTAT1d using primers STIPE-ISH and pT7.5R (SI Appendix, Table S5) was digested using *Bam*HI and *Pst*I and cloned into similarly digested pUNIPROM (57). Plasmid pBADTatABChis codes for *tatABC* with a hexahistag coding sequence at the 3' end of *tatC* in pBAD24 (58). It was constructed following amplification of *tatABChis* from pUNITAT2 (59), digestion with *Nco*I and *Xba*I and cloning into similarly digested pBAD24.

pSUAmiA (36) was used to produce full-length AmiA from a vector specifying chloramphenicol resistance. pSUSufIss-mAmiA was used to produce SufIss-mAmiA and was constructed following separate amplification of DNA encoding the SufI signal sequence including the *sufI* ribosome binding site using primers SufIssFE and SufIssR, and the mature region of AmiA (mAmiA) using primers AmiA-mF and AmiA-mRX from the chromosome, and fusing the two fragments by overlap extension PCR according to reference (60). The resultant DNA fragment was then cloned into the pSU18 vector (61) using *Eco*RI and *Hind*III sites to generate pSUSufIss-mAmiA plasmid. Plasmids pSUSufIssnoH-mAmiA were used for production of

truncated SufIss-mAmiA lacking the signal peptide h-region. It was constructed by removal of codons 11-21 of the SufI signal sequence via Quickchange using pSUSufIss-mAmiA as template with primers SufI-noHF and SufI-noHR. pSUmAmiA was used to produce signal-less AmiA and was constructed as follows. A DNA fragment containing the ribosome binding site of *amiA* and the coding sequence for mature AmiA was amplified using pSUAmiA as template with primers AmiA-nossFE and AmiA-mRX. The DNA fragment was subsequently cloned into pSU18 using *Eco*RI and *Hind*III sites to generate pSUmAmiA. To express the mature domains of AmiA or AmiC from pQE70, DNA covering these regions were amplified with primer pairs mAmiA-SphI-F/AmiAnostopBamHI-R or mAmiC-SphI-F/AmiCnostopBamHI-R, respectively, using chromosomal DNA as template. The DNA fragments were digested with *Sph*I and *Bam*HI and cloned into *Sph*I/*Bgl*II digested pQE70 vector (Qiagen, Manchester, UK). For fractionation experiments, SufI was produced with a C-terminal histag from pQE80 (Qiagen, Manchester, UK). It was cloned by excision of DNA covering a C-terminally his-tagged SufI from pQE60-SufI (62) as an *Nhe*I-*Xho*I fragment and ligation into similarly digested pQE80.

Plasmid pMAK-AupBC was used to introduce the mutations into the AyBCE chromosome and was constructed by amplification of 500 bp of *tatA* upstream DNA from the chromosome of strain AyBCE using primers TatAup1-*Xba*I and TatAup2-*Cla*I, which was cloned into pBluescript KS(+) using *Xba*I and *Cla*I sites to give pKS-Aup. Next a DNA fragment covering the whole of *tatBC* was amplified from the chromosome of AyBCE strain with primers TatA6B7-*Cla*I and TatCrev-*Kpn*I, and cloned into pKS-Aup using *Cla*I and *Kpn*I sites to generate pKS-AupBC. Subsequently the DNA covering the *tatA* upstream sequence along with *tatBC* was excised using *Xba*I and *Kpn*I and cloned into similarly digested pMAK705 (55) to give pMAK-AupBC.

Plasmid pFAT75ΔA-BC, which is a pQE-based plasmid expressing TatB and TatC without a histag (19), and pSufIss-GFPhis, which is a pCFDuet-based plasmid expressing synthetic SufI signal sequence-fused GFP with a histag at its C-terminus under the control of T7 promoter, were used in co-purification experiments. Plasmid pFAT75ΔA-BC-AmiAhis coproduces untagged TatBC along with his-tagged AmiA and was constructed as follows. A DNA fragment

503 covering *amiA* was amplified from MC4100 genomic DNA using primers AmiAFATApaI-F and
504 AmiAnostopBamHI-R, digested with *Apa*I and *Bam*HI and cloned into *Apa*I - *Bgl*II digested
505 pFAT75-SufIhis (47). pFAT75ΔA-BC-mAmiAhis was constructed similarly, using primer
506 mAmiAFATApaI-F and AmiAnostopBamHI-R to amply DNA covering the mature region of
507 AmiA.
508
509 **Mutant library construction and screening**.
510 To screen for Tat signal sequence suppressors, substitutions of the twin arginine sequence of
511 the AmiA signal peptide (to -RD, -RE, -RN, -RQ, -RH, -HH, -KH and –KQ) were constructed
512 in the pSUAmiA plasmid. The resulting plasmids were individually introduced into strain
513 MCDSSAC Δ*tatABC* and each resulting strain served as host to screen an existing *tatB* mutant
514 library (in plasmid pTAT1d, 600,000 individual clones, 0.25% error rate, (38)).
515 To screen for suppressors of the TatC F94Q substitution, three separate mutagenesis
516 libraries, each of which carried the *tatC* F94Q codon substitution, were constructed that
517 contained random mutations in either *tatAB*, codons 1-93 of *tatC* (*tatC*1) or codons 95-258 of
518 *tatC* (*tatC*2), respectively using a modified MEGAWHOP (megaprimer PCR of whole plasmid)
519 method as described (63). DNA fragments of *tatAB*, *tatC1* and *tatC2* containing random
520 mutations were generated using error-prone PCR. Error-prone PCR was carried out in 1x
521 GoTaq buffer, 7mM $MgCl_2$, 0.2 mM dATP, 0.2mM dGTP, 1mM dCTP, 1mM dTTP, 0.4 μM
522 each primer, 0 to 0.1 mM $MnCl_2$, 50 ng pTAT1dCF94Q plasmid as template and 5 U GoTaq®
523 DNA Polymerase (Promega) in a total volume of 50 μl using a PCR program: 94 °C for 2min
524 followed by 20 cycles of incubation at 94 °C for 30s, 50 °C for 30s, and 72 °C for 3min, and a
525 final incubation at 72 °C for 5min. Primer pairs TatA-FB and TatB-RS were used to amplify
526 *tatAB*, TatCm6 and TatC93R to amplify *tatC*1 and TatC95F and TatCR1d were used to amplify
527 *tatC*2. The DNA fragments were then used as megaprimers to amplify the whole plasmid,
528 which was carried out in a 50 μl mixture containing 1x Herculase II reaction buffer, 0.5 mM
529 each dNTP, 100ng pTAT1dCF94Q plasmid as template, 500 ng DNA fragment obtained
530 above as megaprimers and 5 U Herculase II Fusion DNA Polymerase (Agilent) using the PCR

program : incubation at 68 °C for 5min, 95 °C for 2min, followed by 20 cycles of incubation at 95 °C for 30s, 55 °C for 30s, and 68 °C for 6min. The resultant whole plasmid PCR products were digested with *Dpn* I to remove the template DNA and incubated with T4 polynucleotide kinase and T4 DNA ligase to repair the nicks. Finally, the whole plasmids were separately transformed into XL10-Gold® Ultracompetent Cells (Agilent) resulting in three mutagenesis libraries. Subsequent sequencing of 10 randomly selected colonies from each library revealed an average error rate of approximately 2 nucleotides per 1000 base pair. Screening of these three libraries was carried out in strain DADE (Δ*tatABCD*, Δ*tatE*).

For screening experiments the libraries were transformed into the respective host strains and subsequently plated onto solid LB medium containing appropriate antibiotics and 2% SDS for selection. Colonies able to grow under these conditions were isolated, the mutations in the *tat* gene(s) identified by sequencing and retested for growth in the presence and absence of 2% SDS. To further verify isolated candidates, individual mutations were introduced into low copy number plasmid pTAT101 by site-directed mutagenesis and the activity was again assessed on 2% SDS-containing plates.

Protein methods. For co-purification of TatBC-substrate complexes, cultures of strain BL21(DE3) Δ*tatABC* harboring pFAT75ΔA (or a point-substituted variant) and pSufI-GFPhis were incubated at 37°C for 7 hours with shaking, after which they were supplemented with 0.2mM isopropyl β-D-1-thiogalactopyranoside (IPTG) and incubated for a further 17 hours at 37°C. The cells were subsequently harvested and resuspended in 1 x PBS, the fluorescence intensity of the suspension was recorded, after which the cells were re-pelleted, resuspended in 2 x lysis buffer (100 mM NaH_2PO_4 pH 8.0, 600 mM NaCl, 40 mM imidazole, 50 mg lysozyme, 80 U benzonase, and protease inhibitor) and mixed gently at room temperature for one hour. Cells were snap frozen at -80°C, thawed at room temperature and an equivalent amount of 2.5% digitonin was added and the sample gently mixed at room temperature for one hour. Cell debris was pelleted by centrifugation and the supernatant was transferred to a 96-well plate and mixed with 20 µl Ni-NTA Magnetic Agarose Beads (Qiagen) for one hour. After the beads

559 were washed three times with wash buffer (50 mM NaH_2PO_4, pH 8.0, 300 mM NaCl , 40 mM
560 imidazole, 0.03 % digitonin), bound proteins were eluted with 50 µl elution buffer (50 mM
561 NaH_2PO_4, pH 8.0, 300 mM NaCl , 250 mM imidazole, 0.03 % digitonin).
562 *In vivo* disulfide crosslinking was carried out in strain DADE harboring pTAT101 cys less
563 CM205C, as described in (47). Blue-Native PAGE was undertaken according to (47, 64).
564 Subcellular fractionation was according to (65). Preparation of membrane fractions was as
565 described previously (39). For analysis of SufI export, *E. coli* strain DADE harboring wild-type
566 or signal peptide variants of pQE80SufIhis alone or alongside wild-type or TatB variants of
567 pTAT101 was cultured in the presence of 1mM IPTG until OD_{600} of 1 was reached. Samples
568 (equivalent to 150 µl of whole cells from an OD_{600} = 1, or periplasm fractions from the
569 equivalent of 300 µl of cells from an OD_{600} = 1) were separated by SDS PAGE and analysed
570 by Western blot with anti-6X His tag® or anti-RNA polymerase β subunit antibodies
571 (cytoplasmic control protein). For analysis of CueO export, strain MΔBC harbouring wild-type
572 and KK variants of pQE80-CueO alongside wild-type, $tatB^{E8K}$ or $tatB^{F13Y}$ variants of
573 p101C*BCflag were cultured and fractionated as previously described (34). Immunoblotting
574 was according to the methodology of (66), and antibodies to TatA, TatB and TatC have been
575 described previously (47, 67). Anti-6X His tag® antibody (HRP-conjugated) was purchased
576 from Abcam (Cambridge, UK, catalog number ab184607), anti-DnaK mouse monoclonal
577 8E2/2 antibody was also from Abcam (catalog number ab69617) and a mouse monoclonal
578 anti RNA polymerase β-subunit antibody was purchased from NeoClone Biotechnology
579 (Madison, USA; catalog number W0023). Secondary antibodies were goat anti-Rabbit IgG
580 (HRP Conjugate, catalog number 170-6515) or Goat Anti-Mouse IgG (HRP conjugate, catalog
581 number170-6516), both from Biorad (Hemel Hempstead, UK). Immunoreactive bands were
582 visualized with the Clarity Western ECL Substrate Kit (BioRad) and captured either on light-
583 sensitive film or using the GeneGNOME camera (Syngene).
584

585 **Cell permeability experiments**. Cell permeability experiments were performed according to
586 (48). Briefly, cells were grown aerobically at 37°C with 1:100 inoculation of an overnight culture
587 for 2 hours. Production of TatABC harboring TatB variants and of SecY(Δplug)EG was induced
588 by addition of 0.2% arabinose at 37°C for 3 hours. Subsequently, the OD_{600nm} of each sample
589 was normalized using LB, a small volume was withdrawn for Western blotting and equal
590 volumes of each culture were then harvested and resuspended in fractionation buffer (50 mM
591 Tris-HCl buffer, 20% sucrose, pH 7.5, 5 mM EDTA, 0.6 mg/ml lysozyme) and incubated at
592 room temperature for 20min to obtain spheroplasts. The spheroplast samples were then
593 adjusted to the same OD_{600} and a 19-fold excess of 0.616 M xylitol solution was added. The
594 samples were rapidly transferred to a 96-well plate and OD_{600} was measured every 30
595 seconds for 300 seconds.
596
597 **Fluorescence microscopy.** Cells were prepared for fluorescence microscopy and imaged as
598 previously described (47), with the exception that a 550nm LP emission filter was used.
599
600
601

Acknowledgements

This work was supported by the UK Biotechnology and Biological Sciences Research Council (through grants BB/L002531/1 and BB/N014545/1), the UK Medical Research Council (through grants G1001640, K000721 and MR/L000776/1), the Wellcome Trust (through Investigator Award 107929/Z/15/Z to BCB and a Wellcome Trust PhD studentship to SR) and the China Scholarship Council (through a studentship to QH). TP and SML are Wellcome Trust Investigators and TP is a Royal Society/Wolfson merit award holder. We thank Dr Bérengère Ize for her assistance in constructing pQE70-mAmiA and pQE70-mAmiC, Professor Ian Collinson for the gift of pBADplugSecY and Drs Hajra Basit and Mark Wallace for fluorescence microscopy access and advice.

Figure Legends

Figure 1. Isolation of signal sequence suppressors in *tatB*. A. Schematic representation of a twin arginine signal peptide. The signal peptide sequences of *E. coli* Tat substrates SufI and AmiA are given underneath, with residues matching the Tat consensus motif in red, the consecutive arginines in red underline and the signal peptidase cleavage site in black underline. B and C. An example of screening results. Growth of MCDSSAC Δ*tatABC* coproducing the indicated TatB variants (with wild type *tatA* and *tatC*) from pTAT101, alongside B. the HH or C. RE-substituted signal peptide variants of AmiA, on LB agar supplemented with chloramphenicol and kanamycin, with or without the addition of 2% SDS as indicated. An 8μl aliquot of each strain/plasmid combination following aerobic growth to an OD_{600} of 1.0 was spotted and incubated for 16 hr at 37°C.

Figure 2. Isolation of suppressors of the TatC F94Q inactivating substitution. A. Model of *E. coli* TatC (from (47)) showing the location of the F94 and E103 residues (in red) that form part of the signal peptide binding. B., C. and E. Growth of DADE (Δ*tatABCD*, Δ*tatE*) coproducing wild type TatA alongside; B. and C. F94Q-substituted TatC or E. E103A-substituted TatC, and the indicated substitution in TatB from plasmid pTAT101 on LB agar or LB agar containing 2% SDS. D. Structure of *E. coli* TatB (from (68)) with the locations of the TatCF94Q suppressor substitutions shown in red. F. Strain MC4100 Δ*ami*A Δ*amiC* Δ*tatABC* coproducing the indicated TatB variants (with wild type *tatA* and *tatC*) from pTAT101, alongside either a signal peptide variant of SufI lacking the h-region fused to the AmiA mature domain, or the mature AmiA domain alone on LB agar or LB agar containing 1% SDS. For all growth tests, a single colony of each strain/plasmid combination was resuspended in 30μl of PBS and an 8μl aliquot was spotted onto LB agar supplemented with appropriate antibiotics, along with SDS as indicated and incubated for 16 hr at 37°C.

Figure 3. TatB suppressors support export of a Tat substrate with its native signal peptide. *E. coli* strains producing native levels of TatA, TatC and the indicated TatB variants, and overproducing his-tagged CueO with a wild-type (top panel) or KK-substituted (bottom panel) signal peptide were fractionated into whole cell (W), spheroplast (S) and periplasm (P) fractions. Equivalent amounts of each fraction were separated by SDS PAGE and analysed by Western blot with antibodies against CueO and the cytosolic marker DnaK.

Figure 4. The TatB suppressors do not restore signal peptide binding to the TatBC complex. A. C-terminally his-tagged GFP with the wild type (RR) or twin-arginine substituted SufI signal peptide at its N-terminus, as indicated, was purified by magnetic nickel beads from digitonin–treated cell extracts co-expressing TatC along with either wild type TatB or the E8K, F13Y or I36N substituted variants. B. C-terminally his-tagged GFP with the wild type SufI signal peptide at its N-terminus was purified by magnetic nickel beads from digitonin–treated cell extracts co-expressing TatB and TatC with the indicated amino acid substitutions. For A. and B. the elution fractions from each sample were normalized for GFP fluorescence and an equivalent amount of purified SufIss-GFPhis was loaded onto SDS-PAGE (4-15% Mini-PROTEAN® TGX™ precast gradient gel) followed by western blot using TatB and TatC mixed antibodies.

Figure 5. A constitutive disulfide crosslink and aberrant Blue-native PAGE migration induced by a subset of TatB suppressors. A-B. Membranes from *E. coli* strain DADE (Δ*tatABCD* Δ*tatE*) producing the indicated TatB variants alongside wild-type TatA and TatC from plasmid pTAT1d were solubilized by addition of 2% digitonin and analysed by BN-PAGE (4-16% Bis-Tris NativePAGE gels) followed by Western blot with anti-TatA, anti-tatB or anti-TatC antibodies as indicated. 20 μg solubilized membrane was loaded in each lane. C. Membranes from strain DADE producing the indicated TatB variant alongside wild-type TatC from plasmid pTATBC1d were solubilized and analysed as in A-B. D. Whole cells of DADE harboring pTAT101 co-producing either wild type TatA, the M205C single cysteine variant of TatC and the indicated substitution in TatB, or wild type TatA, the TatC F94Q M205C variant

of TatC and the indicated substitution in TatB were subjected to oxidizing (O) or reducing (R) conditions. Where indicated the additional plasmid pQE80-CueO, (producing His-tagged CueO) was also present. Membranes were prepared from equal quantities of cells following treatment and equivalent amounts of material from each sample were resolved by non-reducing SDS-PAGE (12% acrylamide). TatC was visualized by western blotting using an anti-TatC antibody and CueO-His with an anti-His antibody.

Figure 6. The TatB F13Y substitution promotes constitutive oligomerisation of TatA *in vivo*. Fluorescence images of TatA-YFP in representative cells of A. strains AyBCE or $AyBC_{F94Q}E$ (encoding the TatC F94Q substitution in chromosomal *tatC*) in the presence (pAmiA) or absence of plasmid-encoded wild type AmiA, as indicated. Production of AmiA was induced by addition of 1mM IPTG to mid-log cell cultures 45 min before harvesting. B. strains $AyB_{F13Y}CE$ (encoding the TatB F13Y substitution in chromosomal *tatB*) and $AyBC_{F94Q}E$ (encoding the TatB F13Y substitution in chromosomal *tatB*, alongside the TatC F94Q substitution in chromosomal *tatC*). Representative micrographs are shown for each sample; Scale bar: 1 μm.

Figure 7. No detectable leak of xylitol across the cytoplasmic membrane when cells produce Tat translocases harboring TatB suppressors. A. Overnight cultures of *E. coli* strain BW25113 Δ*glpF* Δ*tatABC* harboring pBAD24 encoding TatA and TatC-his along with wild type TatB or each of the L9Q, L10P, F13Y or I36N point substitutions, were subcultured at 1:100 dilution into fresh LB medium containing ampicillin, which was supplemented after 120 min with 0.2% of glucose or arabinose, as indicated. Growth of the strains was followed for a further 6.5h. Error bars represent standard deviation, $n = 3$ (biological replicates). B. The same strain and plasmid combinations as in part A, alongside BW25113 Δ*glpF* harboring pBAD22SecY(Δplug)EG. were subcultured and supplemented with 0.2% of arabinose as described in part A and grown for a further 3 h after which spheroplasts were prepared and incubated in the presence of xylitol. C. An aliquot of each sample producing plasmid-encoded

692 Tat proteins was analysed by SDS PAGE and western blotting to confirm expression of TatA,
693 TatB and TatC-his.

694 **Figure 8. Tat translocases containing TatB suppressor variants may more readily**
695 **transition to the signal peptide-activated state.** Top panel: Model for Tat transport. A signal
696 peptide bound through its n-region to the cytoplasmic surface of TatC (step 1) transitions to a
697 deep binding mode (step 2). The deep insertion of the signal peptide displaces TatB from its
698 resting state binding site on TatC (grey arrow). TatB movement allows polymerisation of TatA
699 to be nucleated (step 3). The substrate passes across the membrane facilitated by the TatA
700 oligomer (step 4). Bottom panel: TatB variants that suppress signal sequence defects
701 (represented as *B**) may be more easily displaced from the resting state binding site. The TatB
702 variants appear to be on a continuum with TatB F13Y pushing the Tat system into an
703 assembled state (step 4), whereas Tat systems harboring the weaker suppressing variants
704 are more likely to correspond to step 3.

705

706 **References**

707 1. Collinson I, Corey RA, Allen WJ (2015) Channel crossing: how are proteins shipped
708 across the bacterial plasma membrane? *Philos Trans R Soc Lond B Biol Sci*
709 370(1679). pii: 20150025. doi: 10.1098/rstb.2015.0025.
710
711 2. Denks K*, et al.* (2014) The Sec translocon mediated protein transport in prokaryotes
712 and eukaryotes. *Mol Membrane Biol* 31(2-3):58-84.
713
714 3. Emr SD, Hanley-Way S, Silhavy TJ (1981) Suppressor mutations that restore export
715 of a protein with a defective signal sequence. *Cell* 23(1):79-88.
716
717 4. Oliver DB, Beckwith J (1981) *E. coli* mutant pleiotropically defective in the export of
718 secreted proteins. *Cell* 25(3):765-772.
719
720 5. Van den Berg B*, et al.* (2004) X-ray structure of a protein-conducting channel. *Nature*
721 427(6969):36-44.
722
723 6. Smith MA, Clemons WM, Jr., DeMars CJ, Flower AM (2005) Modeling the effects of
724 prl mutations on the *Escherichia coli* SecY complex. *J Bacteriol* 187(18):6454-6465.
725
726 7. Trueman SF, Mandon EC, Gilmore R (2011) Translocation channel gating kinetics
727 balances protein translocation efficiency with signal sequence recognition fidelity. *Mol*
728 *Biol Cell* 22(17):2983-2993.
729
730 8. Emr SD, Schwartz M, Silhavy TJ (1978) Mutations altering the cellular localization of
731 the phage lambda receptor, an *Escherichia coli* outer membrane protein. *Proc Natl*
732 *Acad Sci USA* 75(12):5802-5806.
733
734 9. Gouridis G, Karamanou S, Gelis I, Kalodimos CG, Economou A (2009) Signal peptides
735 are allosteric activators of the protein translocase. *Nature* 462(7271):363-367.
736
737 10. Cline K (2015) Mechanistic Aspects of Folded Protein Transport by the Twin Arginine
738 Translocase (Tat). *J Biol Chem* 290(27):16530-16538.
739
740 11. Berks BC (2015) The twin-arginine protein translocation pathway. *Ann Rev Biochem*
741 84:843-864.
742
743 12. Chaddock AM*, et al.* (1995) A new type of signal peptide: central role of a twin-arginine
744 motif in transfer signals for the delta pH-dependent thylakoidal protein translocase.
745 *EMBO J* 14(12):2715-2722.
746
747 13. Berks BC (1996) A common export pathway for proteins binding complex redox
748 cofactors? *Mol Microbiology* 22(3):393-404.
749
750 14. Weiner JH*, et al.* (1998) A novel and ubiquitous system for membrane targeting and
751 secretion of cofactor-containing proteins. *Cell* 93(1):93-101.
752
753 15. Bogsch EG*, et al.* (1998) An essential component of a novel bacterial protein export
754 system with homologues in plastids and mitochondria. *J Biol Chem* 273(29):18003-
755 18006.
756
757 16. Sargent F*, et al.* (1998) Overlapping functions of components of a bacterial Sec-
758 independent protein export pathway. *EMBO J* 17(13):3640-3650.
759

17. Sargent F, Stanley NR, Berks BC, Palmer T (1999) Sec-independent protein translocation in *Escherichia coli*. A distinct and pivotal role for the TatB protein. *J Biol Chem* 274(51):36073-36082.

18. Bolhuis A, Mathers JE, Thomas JD, Barrett CM, Robinson C (2001) TatB and TatC form a functional and structural unit of the twin-arginine translocase from *Escherichia coli*. *J Biol Chem* 276(23):20213-20219.

19. Tarry MJ*, et al.* (2009) Structural analysis of substrate binding by the TatBC component of the twin-arginine protein transport system. *Proc Natl Acad Sci USA* 106(32):13284-13289.

20. Ma X, Cline K (2010) Multiple precursor proteins bind individual Tat receptor complexes and are collectively transported. *EMBO J* 29(9):1477-1488.

21. Kreutzenbeck P*, et al.* (2007) *Escherichia coli* twin arginine (Tat) mutant translocases possessing relaxed signal peptide recognition specificities. *J Biol Chem* 282(11):7903-7911.

22. Lausberg F*, et al.* (2012) Genetic evidence for a tight cooperation of TatB and TatC during productive recognition of twin-arginine (Tat) signal peptides in *Escherichia coli*. *PLoS ONE* 7(6):e39867.

23. Strauch EM, Georgiou G (2007) *Escherichia coli tatC* mutations that suppress defective twin-arginine transporter signal peptides. *J Mol Biol* 374(2):283-291.

24. Zoufaly S*, et al.* (2012) Mapping precursor-binding site on TatC subunit of twin arginine-specific protein translocase by site-specific photo cross-linking. *J Biol Chem* 287(16):13430-13441.

25. Rollauer SE*, et al.* (2012) Structure of the TatC core of the twin-arginine protein transport system. *Nature* 492(7428):210-214.

26. Ma X, Cline K (2013) Mapping the signal peptide binding and oligomer contact sites of the core subunit of the pea twin arginine protein translocase. *Plant cell* 25(3):999-1015.

27. Alami M*, et al.* (2003) Differential interactions between a twin-arginine signal peptide and its translocase in *Escherichia coli*. *Mol Cell* 12(4):937-946.

28. Gerard F, Cline K (2006) Efficient twin arginine translocation (Tat) pathway transport of a precursor protein covalently anchored to its initial cpTatC binding site. *J Biol Chem* 281(10):6130-6135.

29. Blummel AS, Haag LA, Eimer E, Muller M, Frobel J (2015) Initial assembly steps of a translocase for folded proteins. *Nature Comms* 6:7234. doi: 10.1038/ncomms8234.

30. Gerard F, Cline K (2007) The thylakoid proton gradient promotes an advanced stage of signal peptide binding deep within the Tat pathway receptor complex. *J Biol Chem* 282(8):5263-5272.

31. Mori H, Cline K (2002) A twin arginine signal peptide and the pH gradient trigger reversible assembly of the thylakoid [Delta]pH/Tat translocase. *J Cell Biol* 157(2):205-210.

32. Dabney-Smith C, Mori H, Cline K (2006) Oligomers of Tha4 organize at the thylakoid Tat translocase during protein transport. *J Biol Chem* 281(9):5476-5483.

33. Dabney-Smith C, Cline K (2009) Clustering of C-terminal stromal domains of Tha4 homo-oligomers during translocation by the Tat protein transport system. *Mol Biol Celll* 20(7):2060-2069.

34. Alcock F*, et al.* (2013) Live cell imaging shows reversible assembly of the TatA component of the twin-arginine protein transport system. *Proc Natl Acad Sci USA* 110(38):E3650-3659.

35. Rose P, Frobel J, Graumann PL, Muller M (2013) Substrate-dependent assembly of the Tat translocase as observed in live *Escherichia coli* cells. *PLoS ONE* 8(8):e69488.

36. Ize B, Stanley NR, Buchanan G, Palmer T (2003) Role of the *Escherichia coli* Tat pathway in outer membrane integrity. *Mol Microbiol* 48(5):1183-1193.

37. Keller R, de Keyzer J, Driessen AJ, Palmer T (2012) Co-operation between different targeting pathways during integration of a membrane protein. *Journal Cell Biol* 199(2):303-315.

38. Maldonado B*, et al.* (2011) Characterisation of the membrane-extrinsic domain of the TatB component of the twin arginine protein translocase. *FEBS Lett* 585(3):478-484.

39. Kneuper H*, et al.* (2012) Molecular dissection of TatC defines critical regions essential for protein transport and a TatB-TatC contact site. *Mol Microbiol* 85(5):945-961.

40. Holzapfel E*, et al.* (2007) The entire N-terminal half of TatC is involved in twin-arginine precursor binding. *Biochemistry* 46(10):2892-2898.

41. Buchanan G*, et al.* (2002) Functional complexity of the twin-arginine translocase TatC component revealed by site-directed mutagenesis. *Mol Microbiol* 43(6):1457-1470.

42. Wexler M*, et al.* (2000) TatD is a cytoplasmic protein with DNase activity. No requirement for TatD family proteins in sec-independent protein export. *J Biol Chem* 275(22):16717-16722.

43. Richter S, Bruser T (2005) Targeting of unfolded PhoA to the TAT translocon of *Escherichia coli*. *J Biol Chem* 280(52):42723-42730.

44. Oates J*, et al.* (2005) The *Escherichia coli* twin-arginine translocation apparatus incorporates a distinct form of TatABC complex, spectrum of modular TatA complexes and minor TatAB complex. *J Mol Biol* 346(1):295-305.

45. Gohlke U*, et al.* (2005) The TatA component of the twin-arginine protein transport system forms channel complexes of variable diameter. *Proc Natl Acad Sci USA* 102(30):10482-10486.

46. Aldridge C, Ma X, Gerard F, & Cline K (2014) Substrate-gated docking of pore subunit Tha4 in the TatC cavity initiates Tat translocase assembly. *J Cell Biol* 205(1):51-65.

47. Cléon F*, et al.* (2015) The TatC component of the twin-arginine protein translocase functions as an obligate oligomer. *Mol Microbiol* 98(1):111-129.

48. Park E, Rapoport TA (2011) Preserving the membrane barrier for small molecules during bacterial protein translocation. *Nature* 473(7346):239-242.

49. Dalal K, Duong F (2009) The SecY complex forms a channel capable of ionic discrimination. *EMBO Rep* 10(7):762-768.

50 Alcock F, *et al.* (2016) Assembling the Tat protein translocase. Elife. pii: e20718. doi: 10.7554/eLife.20718.

51. Taubert J*, et al.* (2015) TatBC-independent TatA/Tat substrate interactions contribute to transport efficiency. *PLoS ONE* 10(3):e0119761.

52. Lee PA*, et al.* (2006) Cysteine-scanning mutagenesis and disulfide mapping studies of the conserved domain of the twin-arginine translocase TatB component. *J Biol Chem* 281(45):34072-34085.

53. Baba T*, et al.* (2006) Construction of *Escherichia coli* K-12 in-frame, single-gene knockout mutants: the Keio collection. *Mol Syst Biol* 2:2006 0008.

54. Cherepanov PP, Wackernagel W (1995) Gene disruption in *Escherichia coli*: TcR and KmR cassettes with the option of Flp-catalyzed excision of the antibiotic-resistance determinant. *Gene* 158(1):9-14.

55. Hamilton CM, Aldea M, Washburn BK, Babitzke P, Kushner SR (1989) New method for generating deletions and gene replacements in *Escherichia coli*. *J Bacteriol* 171(9):4617-4622.

56. Orriss GL*, et al.* (2007) TatBC, TatB, and TatC form structurally autonomous units within the twin arginine protein transport system of *Escherichia coli*. *FEBS Lett* 581(21):4091-4097.

57. Jack RL*, et al.* (2004) Coordinating assembly and export of complex bacterial proteins. *EMBO J* 23(20):3962-3972.

58. Guzman LM, Belin D, Carson MJ, Beckwith J (1995) Tight regulation, modulation, and high-level expression by vectors containing the arabinose P_{BAD} promoter. *J Bacteriol* 177(14):4121-4130.

59. McDevitt CA, Hicks MG, Palmer T, Berks BC (2005) Characterisation of Tat protein transport complexes carrying inactivating mutations. *Biochem Biophys Res Comm* 329(2):693-698.

60. Heckman KL, Pease LR (2007) Gene splicing and mutagenesis by PCR-driven overlap extension. *Nat Protoc* 2(4):924-932.

61. Bartolome B, Jubete Y, Martinez E, de la Cruz F (1991) Construction and properties of a family of pACYC184-derived cloning vectors compatible with pBR322 and its derivatives. *Gene* 102(1):75-78.

62. Tarry, M, et al (2009) The *Escherichia coli* cell division protein and model Tat substrate SufI (FtsP) localizes to the septal ring and has a multicopper oxidase-like structure*. J Mol Biol* 386(2): 504-519.

63. Miyazaki K, Takenouchi M (2002) Creating random mutagenesis libraries using megaprimer PCR of whole plasmid. *Biotechni* 33(5):1033-1034, 1036-1038.

64. Wittig I, Braun HP, Schagger H (2006) Blue native PAGE. *Nat Protoc* 1(1):418-428.

65. Palmer T, Berks BC, Sargent F (2010) Analysis of Tat targeting function and twin-arginine signal peptide activity in *Escherichia coli*. *Methods Mol Biol* 619:191–216.

66. Towbin H, Staehelin T, Gordon J (1979) Electrophoretic transfer of proteins from polyacrylamide gels to nitrocellulose sheets: procedure and some applications. *Proc Natl Acad Sci USA* 76(9):4350-4354.

67. Sargent F*, et al.* (2001) Purified components of the *Escherichia coli* Tat protein transport system form a double-layered ring structure. *Eur J Biochem / FEBS* 268(12):3361-3367.

68. Zhang Y, Wang L, Hu Y, Jin C (2014) Solution structure of the TatB component of the twin-arginine translocation system. *Biochim Biophys Acta* 1838(7):1881-1888.

A

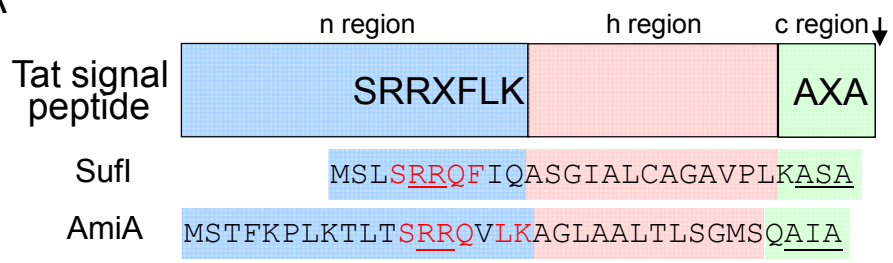

B

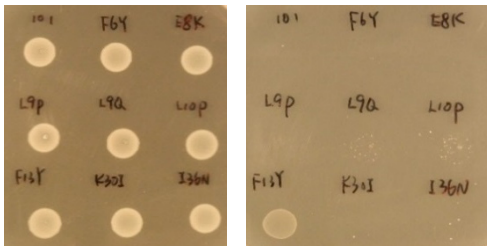

WT TatB	TatB F6Y	TatB E8K
TatB L9P	TatB L9Q	TatB L10P
TatB F13Y	TatB K30I	TatB I36N

AmiAss-HH

C

	WT TatB	*tat*	
TatB F6Y	TatB E8K	TatB L9P	TatB L9Q
TatB L10P	TatB F13Y	TatB K30I	TatB I36N

AmiAss-RE

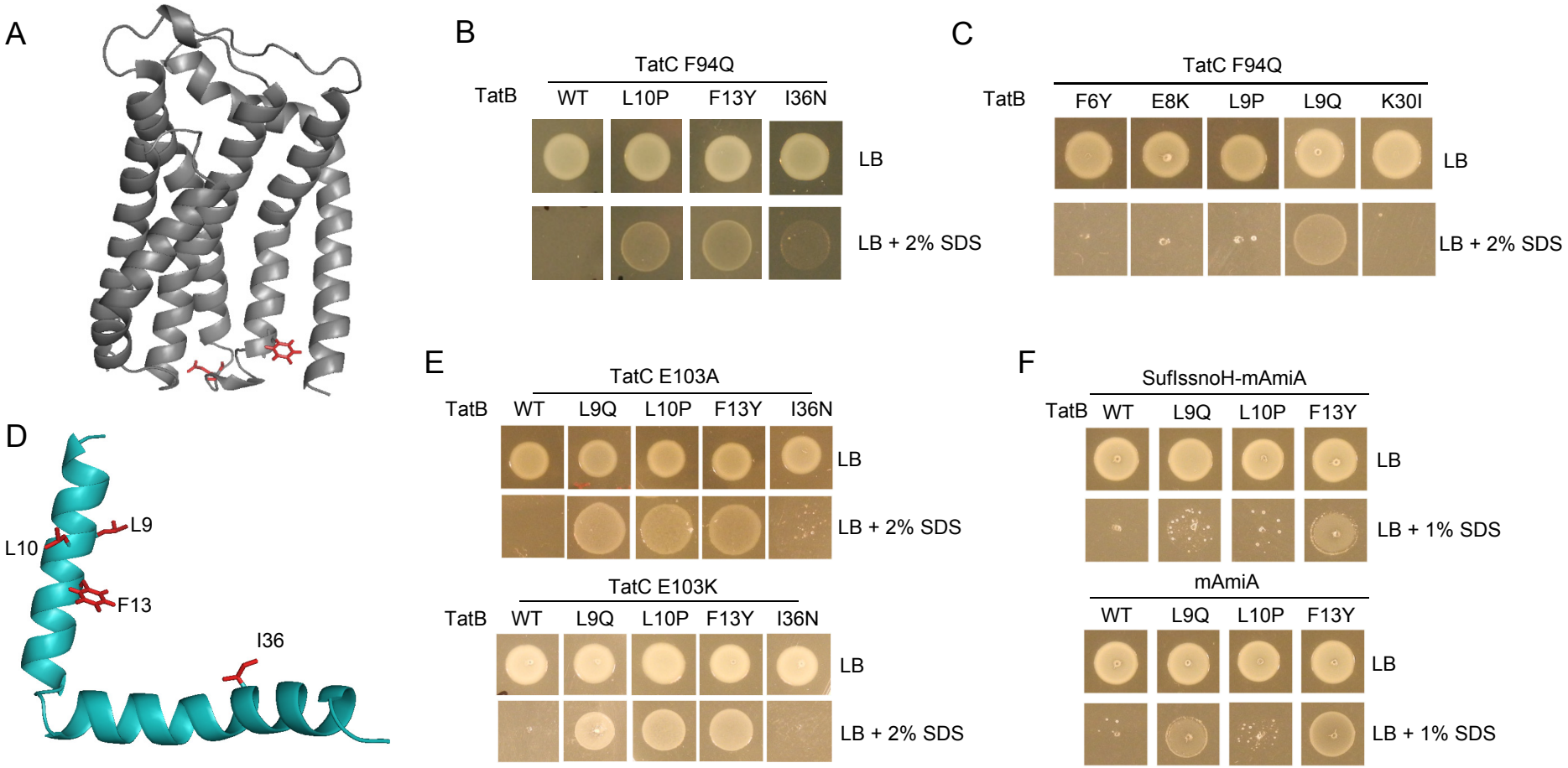
A
B
TatC F94Q
TatB
WT
L10P
F13Y
I36N
LB
LB + 2% SDS
C
TatC F94Q
TatB
F6Y
E8K
L9P
L9Q
K30I
LB
LB + 2% SDS
D
L9
L10
F13
I36
E
TatC E103A
TatB
WT
L9Q
L10P
F13Y
I36N
LB
LB + 2% SDS
TatC E103K
TatB
WT
L9Q
L10P
F13Y
I36N
LB
LB + 2% SDS
F
SufIssnoH-mAmiA
TatB
WT
L9Q
L10P
F13Y
LB
LB + 1% SDS
mAmiA
WT
L9Q
L10P
F13Y
LB
LB + 1% SDS

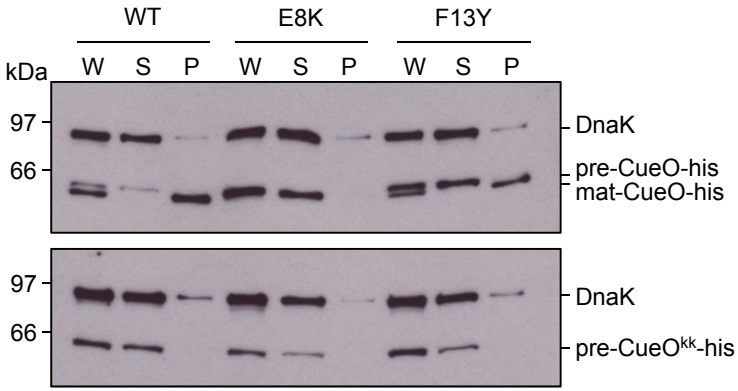
WT
E8K
F13Y
kDa
W S P W S P W S P
97
66
DnaK
pre-CueO-his
mat-CueO-his
97
66
DnaK
pre-CueO^{kk}-his

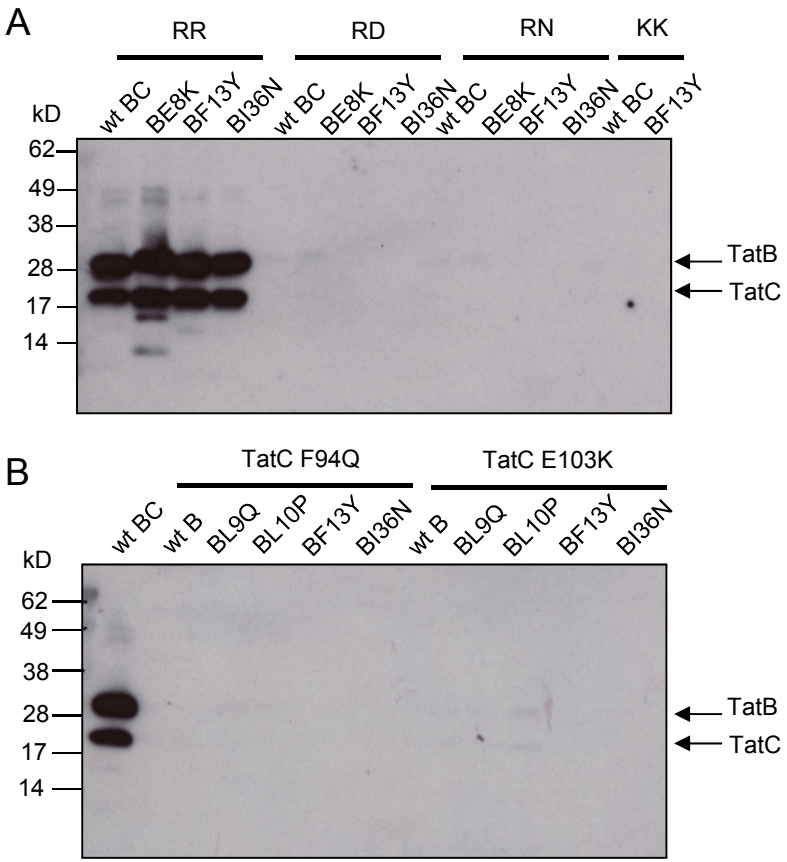
A
RR
RD
RN
KK
kD
wt BC
BE8K
BF13Y
BI36N
wt BC
BE8K
BF13Y
BI36N
wt BC
BE8K
BF13Y
BI36N
wt BC
BF13Y
62
49
38
28
17
14
TatB
TatC
B
TatC F94Q
TatC E103K
kD
wt BC
wt B
BL9Q
BL10P
BF13Y
BI36N
wt B
BL9Q
BL10P
BF13Y
BI36N
62
49
38
28
17
14
TatB
TatC

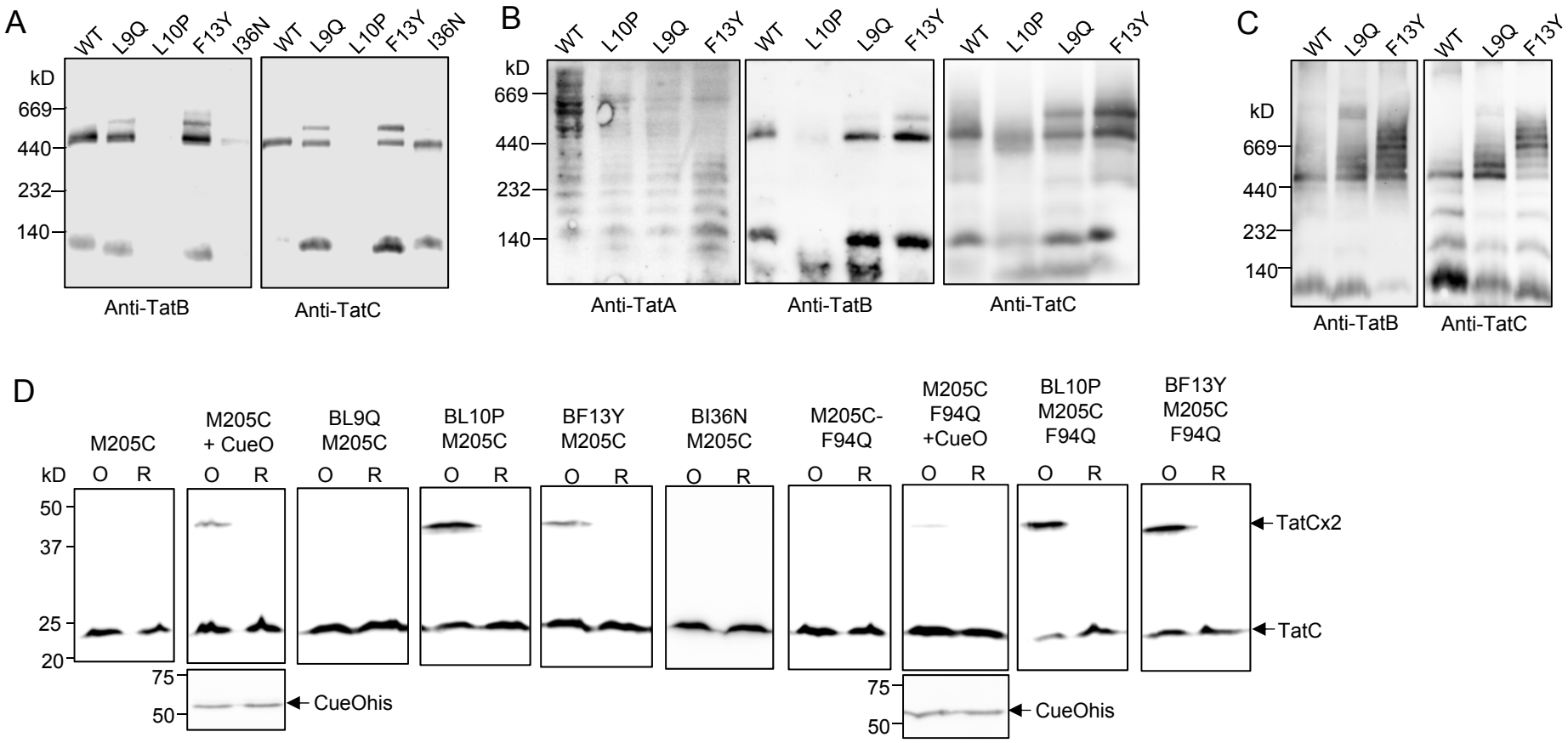
A
WT
L9Q
L10P
F13Y
I36N
kD
669
440
232
140
Anti-TatB
Anti-TatC
B
Anti-TatA
Anti-TatB
Anti-TatC
C
D
M205C
M205C + CueO
BL9Q M205C
BL10P M205C
BF13Y M205C
BI36N M205C
M205C- F94Q
M205C F94Q +CueO
BL10P M205C F94Q
BF13Y M205C F94Q
O
R
50
37
25
20
75
TatCx2
TatC
CueOhis

A

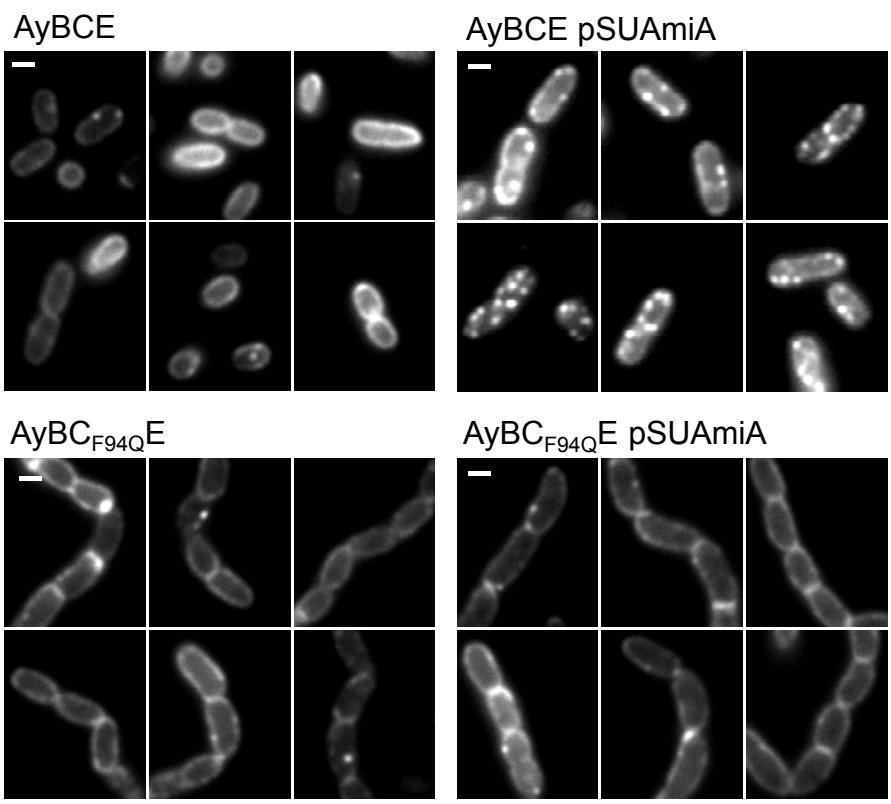
AyBCE
AyBCE pSUAmiA
AyBC$_{F94Q}$E
AyBC$_{F94Q}$E pSUAmiA

B

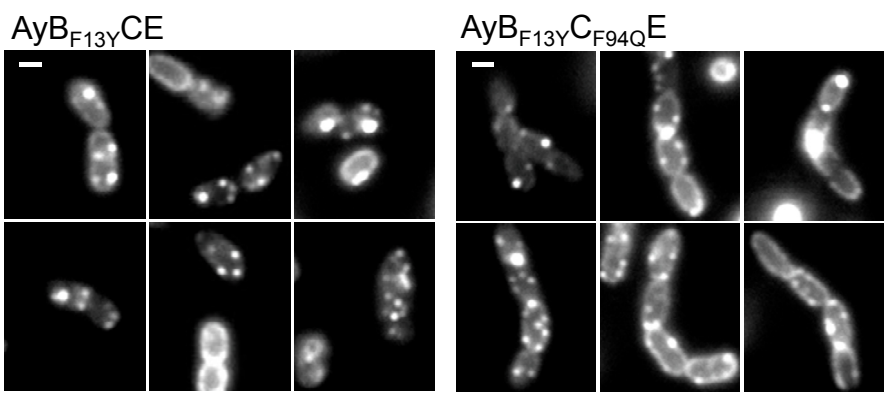
AyB$_{F13Y}$CE
AyB$_{F13Y}$C$_{F94Q}$E

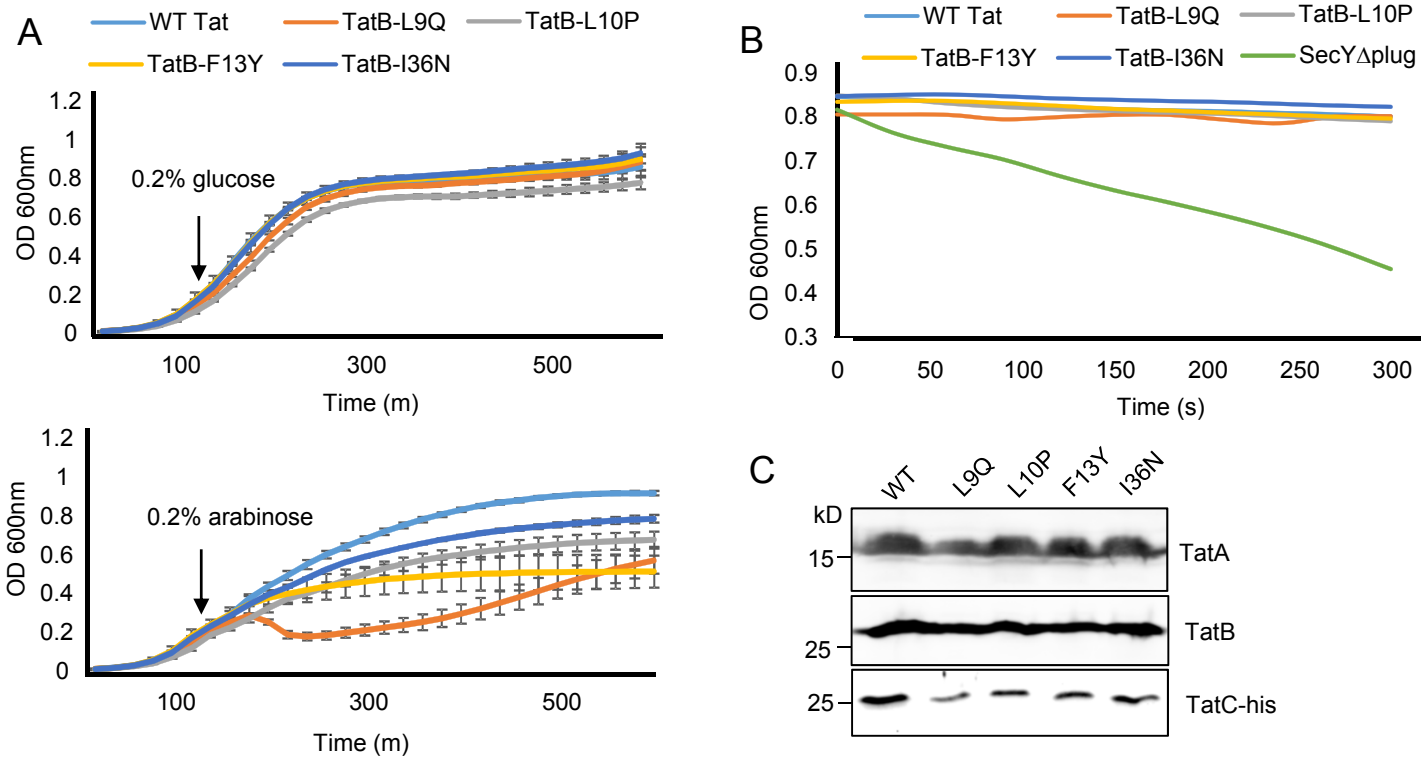
A
WT Tat
TatB-L9Q
TatB-L10P
TatB-F13Y
TatB-I36N
OD 600nm
0.2% glucose
Time (m)
0.2% arabinose
B
SecYΔplug
Time (s)
C
WT
L9Q
L10P
F13Y
I36N
kD
15
25
25
TatA
TatB
TatC-his

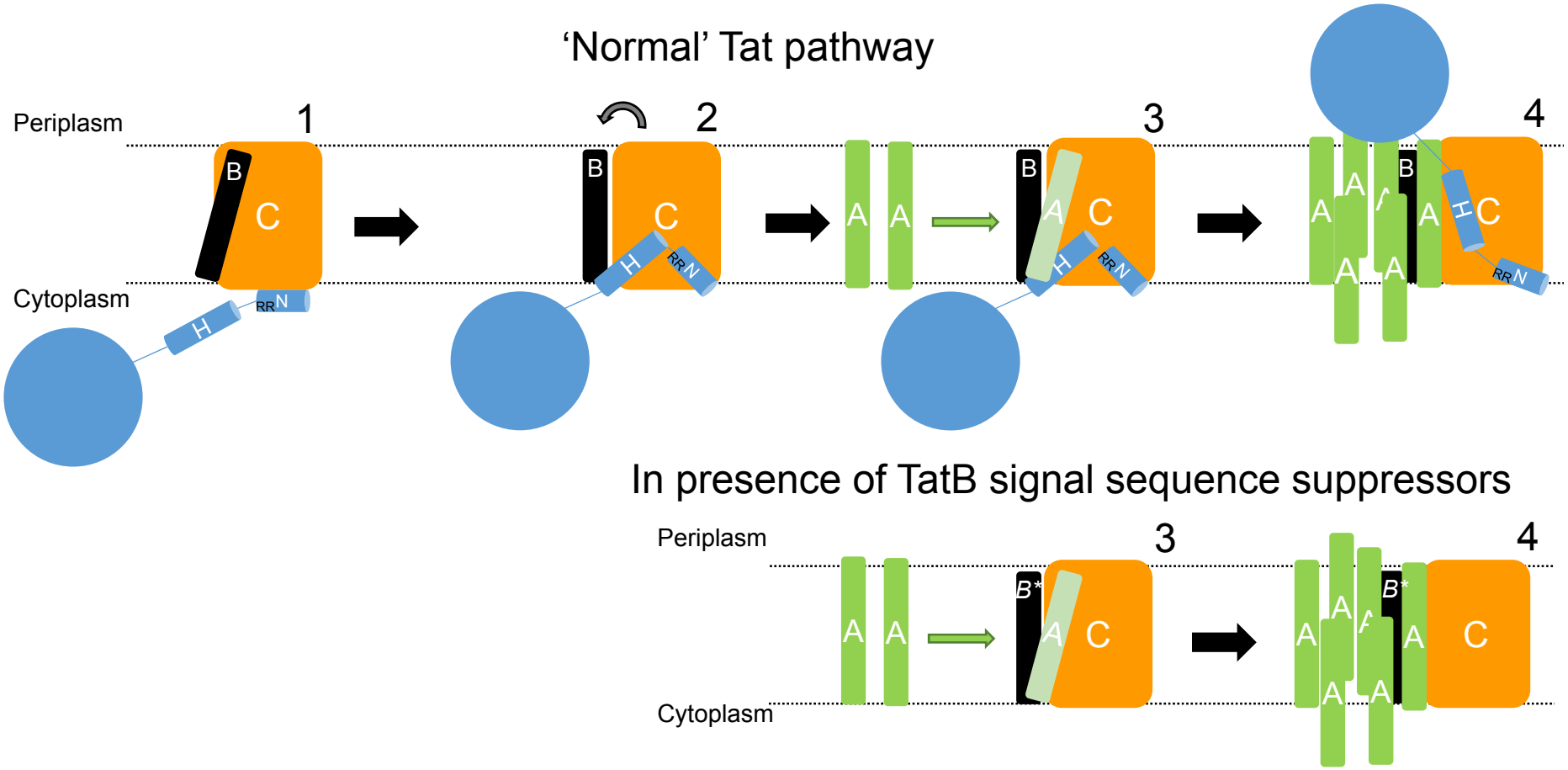
‘Normal’ Tat pathway
Periplasm
Cytoplasm
1
2
3
4
B
C
H
RR
N
A
A
A
A
A
A
In presence of TatB signal sequence suppressors
Periplasm
Cytoplasm
3
4
B*
A
A
A
A
A
A
C

A signal sequence suppressor mutant that stabilizes an assembled state of the twin arginine translocase

Qi Huang, Felicity Alcock, Holger Kneuper, Justin C. Deme[3], Sarah Rollauer, Susan M. Lea, Ben C. Berks and Tracy Palmer

SUPPORTING INFORMATION

SI APPENDIX

Clone	TatB substitution/s
BRE1	L9Q K103R
BRE2*	L9Q
BRN2	L9Q Q134V
BRN3*	L9Q
BRN4	L10P V12M
BRN5	L9P
BRQ1*	K30I K65R N99D
BRQ2*	K30I K65R N99D
BRQ3*	I36N S41T
BRQ4	L9Q T72A
BRQ5*	I36N S41T
BRH1	L9Q N73K
BRH2	E8K L71H
BRH4	F13Y P138L K159R
BRH5*	F13Y
BRH6*	F13Y
BRH7*	L9Q
BRH8	F6Y V32A A69V
BRH9*	F13Y
BKQ1*	F13Y

Table S1. Clones isolated from a *tatB* mutant library following screening for suppression of transport defects of inactive signal peptides. The BRE, BRN, BRQ, BRH, BHH, BKH or BKQ clone nomenclature signify substitutions isolated following screening against RE, RN or KQ variants of the AmiA signal peptide RR motif, respectively.

*identical clones

Clone	TatAB substitution/s
AB-1	TatA K23N,TatB I36N, TatB N119I, TatB S164C
AB-5	TatB L10P
AB-16	TatB L10P, TatB N73Y
AB-157	TatB F13Y
AB-172	TatA A60E, TatA A76R, TatB F13Y

Table S2. Clones isolated from a *tatAB* mutant library following screening for suppression of the transport defect arising from the TatC F94Q substitution.

Strain	Relevant genotype	Source
JM109	*end*A1, *rec*A1, *gyr*A96, *thi, hsd*R17 (r_k^-, m_k^+), *rel*A1, *sup*E44, Δ(*lac-pro*AB), [F´ *tra*D36, *pro*AB, *laq*I^{q}ZΔM15]	Promega
XL10-gold	Tet^{r}Δ(*mcrA*)*183* Δ(*mcrCB-hsdSMR-mrr*)*173 endA1 supE44 thi-1 recA1 gyrA96 relA1 lac Hte* [F´ *proAB lacI*^{q}*ZDM15* Tn*10* (Tet^r) Amy Cam^r]	Agilent
MC4100	F-Δ*lacU169 araD139 rpsL150 relA1 ptsF rbs flbB5301*	(1)
DADE	As MC4100, Δ*tatABC*, Δ*tatE*	(2)
DADE-P	as DADE*, pcnB1 zad*-981*::*Tn*10*d (Kan^r)	(3)
MΔBC	MC4100 Δ*tatBC*	(4)
MCDSSAC Δ*tatABC*	MC4100, *amiA*Δ2-33 *amiC*Δ2-32, Δ*tatABC*::Apra	(5)
MC4100 Δ*amiA* Δ*amiC* Δ*tatABC*	MC4100, Δ*amiA*, Δ*amiC*, Δ*tatABC*::Apra	This work
AyBCE	MC4100 Δ*tatA*, *attB*::P$_{tatA}$*tatA-EAK-eyfp*$_{A206K}$	(4)
AyBCE (*tatB*$_{L9Q}$)	As AyBCE, *tatB*$_{L9Q}$	This work
AyBCE (*tatB*$_{L10P}$)	As AyBCE, *tatB*$_{L10P}$	This work
AyBCE (*tatB*$_{F13Y}$)	As AyBCE, *tatB*$_{F13Y}$	This work
AyBCE (*tatB*$_{I36N}$)	As AyBCE, *tatB*$_{I36N}$	This work
AyBCE (*tatC*$_{F94Q}$)	As AyBCE, *tatC*$_{F94Q}$	This work
AyBCE (*tatB*$_{L9Q}$ *tatC*$_{F94Q}$)	As AyBCE (*tatB*$_{L9Q}$, *tatC*$_{F94Q}$)	This work
AyBCE (*tatB*$_{L10P}$ *tatC*$_{F94Q}$)	As AyBCE (*tatB*$_{L10P}$, *tatC*$_{F94Q}$)	This work
AyBCE (*tatB*$_{F13Y}$ *tatC*$_{F94Q}$)	As AyBCE (*tatB*$_{F13Y}$, *tatC*$_{F94Q}$)	This work
AyBCE (*tatB*$_{I36N}$ *tatC*$_{F94Q}$)	As AyBCE (*tatB*$_{I36N}$, *tatC*$_{F94Q}$)	This work
BL21(DE3) Δ*tatABC*	BL21(DE3), Δ*tatABC*::Apra	This work
BW25113	*lacI*^{q} *rrnB*$_{T14}$ Δ*lacZ*$_{WJ16}$ *hsdR514* Δ*araBAD*$_{AH33}$ Δ*rhaBA D*$_{LD78}$	(6)
BW25113 Δ*glpF* Δ*tatABC*	BW25113, Δ*glpF*, Δ*tatABC*::Apra	This work

Table S3. Strains used and constructed in this study.

Plasmid	Relevant genotype	Source
pTAT101	Low copy number vector expressing TatABC under the control of *tat* promoter. Kan^r.	(7)
pTH19kr	Low copy-number cloning vector. Backbone of pTAT101.	(8)
pTAT101-BF6Y	As pTAT101, TatB F6Y exchange	This work
pTAT101-BE8K	As pTAT101, TatB E8K exchange	This work
pTAT101-BL9P	As pTAT101, TatB L9P exchange	This work
pTAT101-BL9Q	As pTAT101, TatB L9Q exchange	This work
pTAT101-BL10P	As pTAT101, TatB L10P exchange	This work
pTAT101-BF13Y	As pTAT101, TatB F13Y exchange	This work
pTAT101-BK30I	As pTAT101, TatB K30I exchange	This work
pTAT101-BI36N	As pTAT101, TatB I36N exchange	This work
pTAT101-CF94Q	As pTAT101, TatC F94Q exchange	This work
pTAT101-CF94A	As pTAT101, TatC F94A exchange	This work
pTAT101-CF94D	As pTAT101, TatC F94D exchange	This work
pTAT101-CF94G	As pTAT101, TatC F94G exchange	This work
pTAT101-CF94K	As pTAT101, TatC F94K exchange	This work
pTAT101-CF94P	As pTAT101, TatC F94P exchange	This work
pTAT101-CF94R	As pTAT101, TatC F94R exchange	This work
pTAT101-CF94S	As pTAT101, TatC F94S exchange	This work
pTAT101-CF94Q-BF6Y	As pTAT101-CF94Q, TatB F6Y exchange	This work
pTAT101-CF94Q-BE8K	As pTAT101-CF94Q, TatB E8K exchange	This work
pTAT101-CF94Q-BL9P	As pTAT101-CF94Q, TatB L9P exchange	This work
pTAT101-CF94Q-BL9Q	As pTAT101-CF94Q, TatB L9Q exchange	This work
pTAT101-CF94Q-BL10Q	As pTAT101-CF94Q, TatB L10P exchange	This work
pTAT101-CF94Q-BF13Y	As pTAT101-CF94Q, TatB F13Y exchange	This work
pTAT101-CF94Q-BK30I	As pTAT101-CF94Q, TatB K30I exchange	This work
pTAT101-CF94Q-BI36N	As pTAT101-CF94Q, TatB I36N exchange	This work
pTAT101-BL9Q F13Y	As pTAT101, TatB L9Q, F13Y exchange	This work
pTAT101-BL10P F13Y	As pTAT101, TatB L10P, F13Y exchange	This work
pTAT101-BL9Q I36N	As pTAT101, TatB L9Q, I36N exchange	This work
pTAT101-BL10P I36N	As pTAT101, TatB L10P, I36N exchange	This work
pTAT101-CE103A	As pTAT101, TatC E103A exchange	This work
pTAT101-CE103A-BL9Q	As pTAT101-CE103A, TatB L9Q exchange	This work
pTAT101-CE103A-BL10P	As pTAT101-CE103A, TatB L10P exchange	This work
pTAT101-CE103A-BF13Y	As pTAT101-CE103A, TatB F13Y exchange	This work
pTAT101-CE103A-BI36N	As pTAT101-CE103A, TatB I36N exchange	This work
pTAT101-CE103K	As pTAT101, TatC E103K exchange	(7)
pTAT101-CE103K-BL9Q	As pTAT101-CE103K, TatB L9Q exchange	This work
pTAT101-CE103K-BL10P	As pTAT101-CE103K, TatB L10P exchange	This work

pTAT101-CE103K-BF13Y	As pTAT101-CE103A, TatB F13Y exchange	This work
pTAT101-CE103K-BI36N	As pTAT101-CE103A, TatB I36N exchange	This work
pTAT101-CP48L	As pTAT101, TatC P48L exchange	(9)
pTAT101-CP48L- BL9Q	As pTAT101-CP48L, TatB L9Q exchange	This work
pTAT101-CP48L - BL10P	As pTAT101-CP48L, TatB L10P exchange	This work
pTAT101-CP48L - BF13Y	As pTAT101-CP48L, TatB F13Y exchange	This work
pTAT101-CM59K	As pTAT101, TatC M59K exchange	(9)
pTAT101-CM59K-BL9Q	As pTAT101-CM59K, TatB L9Q exchange	This work
pTAT101-CM59K - BL10P	As pTAT101-CM59K, TatB L10P exchange	This work
pTAT101-CM59K - BF13Y	As pTAT101-CM59K, TatB F13Y exchange	This work
pTAT101-CV145E	As pTAT101, TatC V145E exchange	(9)
pTAT101-CV145E-BL9Q	As pTAT101-CV145E, TatB L9Q exchange	This work
pTAT101-CV145E - BL10P	As pTAT101-CV145E, TatB L10P exchange	This work
pTAT101-CV145E - BF13Y	As pTAT101-CV145E, TatB F13Y exchange	This work
pTAT101-CD211K	As pTAT101, TatC D211K exchange	This work
pTAT101-CD211K-BL9Q	As pTAT101-CD211K, TatB L9Q exchange	This work
pTAT101-CD211K - BL10P	As pTAT101-CD211K, TatB L10P exchange	This work
pTAT101-CD211K - BF13Y	As pTAT101-CD211K, TatB F13Y exchange	This work
pTAT101-CQ215K	As pTAT101, TatC Q215K exchange	This work
pTAT101-CQ215K-BL9Q	As pTAT101-CQ215K, TatB L9Q exchange	This work
pTAT101-CQ215K - BL10P	As pTAT101-CQ215K, TatB L10P exchange	This work
pTAT101-CQ215K - BF13Y	As pTAT101-CQ215K, TatB F13Y exchange	This work
pTAT101 cys less	As pTAT101, All 4 cys codons in *tatC* substituted with ala	(9)
pTAT101 cys less CM205C	As pTAT101 cys less, TatC M205C exchange	(9)
pTAT101 cys less BL9Q CM205C	As pTAT101 cys less CM205C, TatB L9Q exchange	This work
pTAT101 cys less BL10P CM205C	As pTAT101 cys less CM205C, TatB L10P exchange	This work
pTAT101 cys less BF13Y CM205C	As pTAT101 cys less CM205C, TatB F13Y exchange	This work
pTAT101 cys less BI36N CM205C	As pTAT101 cys less CM205C, TatB I36N exchange	This work
pTAT101 cys less CF94Q M205C	As pTAT101 cys less CM205C, TatC F94Q	This work
pTAT101 cys less BL10P CF94Q M205C	As pTAT101 cys less CF94Q M205C, TatB L10P	This work

pTAT101 cys less BF13Y CF94Q M205C	As pTAT101 cys less CF94Q M205C, TatB F13Y	This work
pQE80-CueO	As pQE80, carrying *cueO*$_{his}$	(4)
pQE80-CueO^{KK}h	As pQE80-CueO, CueO R3K, R4K exchange	(4)
pTAT1d	Medium copy number vector expressing TatABC under the control of *tat* promoter. Amp^r.	(10)
pUNIPROM	pT7.5 vector carrying a *tat* promoter. Backbone of pTAT1d	(11)
pTAT1d-CF94Q	As pTAT1d, TatC F94Q exchange	This work
pTAT1d-CF94A	As pTAT1d, TatC F94A exchange	This work
pTAT1d-CF94D	As pTAT1d, TatC F94D exchange	This work
pTAT1d-CF94G	As pTAT1d, TatC F94G exchange	This work
pTAT1d-CF94K	As pTAT1d, TatC F94K exchange	This work
pTAT1d-CF94P	As pTAT1d, TatC F94P exchange	This work
pTAT1d-CF94R	As pTAT1d, TatC F94R exchange	This work
pTAT1d-CF94S	As pTAT1d, TatC F94S exchange	This work
pTAT1d-CF94Q-BL9Q	As pTAT1d-CF94Q, TatB L9Q exchange	This work
pTAT1d-CF94Q-BL10P	As pTAT1d-CF94Q, TatB L10P exchange	This work
pTAT1d-CF94Q-BF13Y	As pTAT1d-CF94Q, TatB F13Y exchange	This work
pTAT1d-CF94Q-BI36N	As pTAT1d-CF94Q, TatB I36N exchange	This work
pTATBC1d	pUNIPROM carrying *tatBC*	This work
pSUAmiA	pSU18 carrying *amiA*	(12)
pSUAmiA-RD	As pSUAmiA, R14D exchange	This work
pSUAmiA-RE	As pSUAmiA, R14E exchange	This work
pSUAmiA-RH	As pSUAmiA, R14H exchange	This work
pSUAmiA-RN	As pSUAmiA, R14N exchange	This work
pSUAmiA-RQ	As pSUAmiA, R14Q exchange	This work
pSUAmiA-KH	As pSUAmiA, R13K, R14H exchange	This work
pSUAmiA-KQ	As pSUAmiA, R13K, R14Q exchange	This work
pSUAmiA-HH	As pSUAmiA, R13H, R14H exchange	This work
pSUSufIss-mAmiA	pSU18, carrying SufIss-mAmiA	This work
pSUSufIss-mAmiA-RD	As pSUSufIss-mAmiA, SufI R6D exchange	This work
pSUSufIss-mAmiA-RE	As pSUSufIss-mAmiA, SufI R6E exchange	This work
pSUSufIss-mAmiA-RH	As pSUSufIss-mAmiA, SufI R6H exchange	This work
pSUSufIss-mAmiA-RN	As pSUSufIss-mAmiA, SufI R6N exchange	This work
pSUSufIss-mAmiA-RQ	As pSUSufIss-mAmiA, SufI R6Q exchange	This work
pSUSufIss-mAmiA-KH	As pSUSufIss-mAmiA, SufI R5K, R6H exchange	This work
pSUSufIss-mAmiA-KQ	As pSUSufIss-mAmiA, SufI R5K, R6Q exchange	This work
pSUSufIss-mAmiA-KK	As pSUSufIss-mAmiA, SufI R5K, R6K exchange	This work
pSUSufIss-mAmiA-HH	As pSUSufIss-mAmiA, SufI R5H, R6H exchange	This work
pSUSufIssnoH-mAmiA	As pSUSufIss-mAmiA, *sufI* Δ11-21	This work
pSUmAmiA	As pSUAmiA, *amiA* Δ2-34	This work
pFAT75ΔA-BC	As pQEABC, but with *tatA* gene in frame deleted	(13)
pFAT75ΔA-BC BE8K	As pFAT75ΔA-BC, TatB E8K exchange	This work
pFAT75ΔA-BC BF13Y	As pFAT75ΔA-BC, TatB F13Y exchange	This work
pFAT75ΔA-BC BI36N	As pFAT75ΔA-BC, TatB BI36N exchange	This work
pFAT75ΔA-BC	As pFAT75ΔA-BC, TatC F94Q exchange	This work

CF94Q		
pFAT75ΔA-BC BL9Q CF94Q	As pFAT75ΔA-BC CF94Q, TatB L9Q exchange	This work
pFAT75ΔA-BC BL10P CF94Q	As pFAT75ΔA-BC CF94Q, TatB L10P exchange	This work
pFAT75ΔA-BC BF13Y CF94Q	As pFAT75ΔA-BC CF94Q, TatB F13Y exchange	This work
pFAT75ΔA-BC BI36NC CF94Q	As pFAT75ΔA-BC CF94Q, TatB I36N exchange	This work
pFAT75ΔA-BC-AmiAhis	As pFAT75ΔA-BC also producing C-terminally his-tagged AmiA	This work
pFAT75ΔA-BC-AmiARDhis	As pFAT75ΔA-BC-AmiAhis, AmiA R14D exchange	This work
pFAT75ΔA-BC-AmiARNhis	As pFAT75ΔA-BC-AmiAhis, AmiA R14N exchange	This work
pFAT75ΔA-BC-AmiAKKhis	As pFAT75ΔA-BC-AmiAhis, AmiA R13K, R14K exchange	This work
pFAT75ΔA-BC-AmiAKQhis	As pFAT75ΔA-BC-AmiAhis, AmiA R13K, R14Q exchange	This work
pFAT75ΔA-BF13YC-AmiAhis	As pFAT75ΔA-BC, TatBF13Y exchange	This work
pFAT75ΔA-BF13YC-AmiARDhis	As pFAT75ΔA-BF13YC-AmiAhis, AmiA R14D exchange	This work
pFAT75ΔA-BF13YC-AmiARNhis	As pFAT75ΔA-BF13YC-AmiAhis, AmiA R14N exchange	This work
pFAT75ΔA-BF13YC-AmiAKKhis	As pFAT75ΔA-BF13YC-AmiAhis, AmiA R13K, R14K exchange	This work
pFAT75ΔA-BF13YC-AmiAKQhis	As pFAT75ΔA-BF13YC-AmiAhis, AmiA R13K, R14Q exchange	This work
pFAT75ΔA-BC-mAmiAhis	As pFAT75ΔA-BC also producing C-terminally his-tagged mature AmiA	This work
pFAT75ΔA-BF13YC-mAmiAhis	As pFAT75ΔA-BC-mAmiAhis, TatBF13Y exchange	This work
pQE70-mAmiA	pQE70 producing C-terminally his-tagged mature AmiA	This work
pQE70-mAmiC	pQE70 producing C-terminally his-tagged mature AmiC	This work
pSufIss-GFPhis	As pCDFDuet-1, carrying synthetic SufI signal sequence-fused GFPhis	This work
pSufIssRD-GFPhis	As pSufIss-GFPhis, SufI R6D exchange	This work
pSufIssRN-GFPhis	As pSufIss-GFPhis, SufI R6N exchange	This work
pSufIssKK-GFPhis	As pSufIss-GFPhis, SufI R5K, R6K exchange	This work
pQE80 suflhis	pQE80 carrying *suflhis*	This work
pQE80 RDsuflhis	pQE80 suflhis SufI R6D exchange	This work
pQE80 RNsuflhis	pQE80 suflhis SufI R6N exchange	This work
pQE80 KQsuflhis	pQE80 suflhis SufI R5K, R6Q exchange	This work
pMAK705	Cloning vector with a temperature-sensitive replicon	(14)
pMAK-AupBC	As pMAK705, carrying 500 bp upstream sequence of *tatA* and *tatBC* sequence	This work
pMAK-AupBC-BL9Q	As pMAK-AupBC, TatB L9Q exchange	This work
pMAK-AupBC-BL10P	As pMAK-AupBC, TatB L10P exchange	This work
pMAK-AupBC-BF13Y	As pMAK-AupBC, TatB F13Y exchange	This work

pMAK-AupBC-BI36N	As pMAK-AupBC, TatB I36N exchange	This work
pMAK-AupBC-CF94Q	As pMAK-AupBC, TatC F94Q exchange	This work
pMAK-AupBC- BL9Q CF94Q	As pMAK-AupBC, TatB L9Q, TatC F94Q exchange	This work
pMAK-AupBC- BL10P CF94Q	As pMAK-AupBC, TatB L10P, TatC F94Q exchange	This work
pMAK-AupBC- BF13Y CF94Q	As pMAK-AupBC, TatB F13Y, TatC F94Q exchange	This work
pMAK-AupBC- BI36N CF94Q	As pMAK-AupBC, TatB I36N, TatC F94Q exchange	This work
pBAD24	Arabinose-inducible protein expression vector	(15)
pBADTatABChis	As pBAD24, carrying *tatABC*his	This work
pBADTatABChis-BL9Q	As pBADTatABChis, TatB L9Q exchange	This work
pBADTatABChis-BL10P	As pBADTatABChis, TatB L10P exchange	This work
pBADTatABChis-BF13Y	As pBADTatABChis, TatB F13Y exchange	This work
pBADTatABChis-BI36N	As pBADTatABChis, TatB I36N exchange	This work
pBAD22SecY(Δplug)EG	pBAD22, producing SecY(Δcodons62-72)EG	Ian Collinson
p101C*TatBC	Low copy vector for expression of *tatBC* from the *tatA* promoter with a modified RBS	(4)
p101C*BCflag	p101C*BC derivative producing TatB and C-terminally flag-tagged TatC	This work
p101C*BCflag E8K	As p101C*BCflag, TatB E8K exchange	This work
p101C*BCflag F13Y	As p101C*BCflag, TatB F13Y exchange	This work

Table S4. Plasmids used and constructed in this study

Primer name	Sequence (5'-3')
AmiARDf	CTCACTTCGCGCGACCAGGTGCTG
AmiARDr	CAGCACCTGGTCGCGCGAAGTGAG
AmiAREf	CTCACTTCGCGCGAACAGGTGCTG
AmiAREr	CAGCACCTGTTCGCGCGAAGTGAG
AmiARNf	CTCACTTCGCGCAACCAGGTGCTG
AmiARNr	CAGCACCTGGTTGCGCGAAGTGAG
AmiARQf	CTCACTTCGCGCCAACAGGTGCTG
AmiARQr	CAGCACCTGTTGGCGCGAAGTGAG
AmiARHf	CTCACTTCGCGCCACCAGGTGCTG
AmiARHr	CAGCACCTGGTGGCGCGAAGTGAG
AmiAHHf	CTCACTTCGCACCACCAGGTGCTG
AmiAHHr	CAGCACCTGGTGGTGCGAAGTGAG
AmiAKHf	CTCACTTCGAAACACCAGGTGCTG
AmiAKHr	CAGCACCTGGTGTTTCGAAGTGAG
AmiAKQf	CTCACTTCGAAACAACAGGTGCTG
suflssFE	CCGGAATTCGTTTTACATGGAGCAAATATG
suflssR	GTTCGTCTTTTGCGCTGGCCTTCAGGG
amiA-mF	GGCCAGCGCAAAAGACGAACTTTTAAAAACC
amiA-mRX	GACTCTAGATTATCGCTT TTTC
AmiAKQr	CAGCACCTGTTGTTTCGAAGTGAG
Suflss-RDf	GTCACTCAGTCGGGATCAGTTCATTCAGGC
Suflss-RDr	GCCTGAATGAACTGATCCCGACTGAGTGAC
Suflss-RHf	GTCACTCAGTCGGCATCAGTTCATTCAGGC
Suflss-RHr	GCCTGAATGAACTGATGCCGACTGAGTGAC
Suflss-RNf	GTCACTCAGTCGGAACCAGTTCATTCAGGC
Suflss-RNr	GCCTGAATGAACTGGTTCCGACTGAGTGAC
Suflss-RQf	GTCACTCAGTCGGCAGCAGTTCATTCAGGC
Suflss-RQr	GCCTGAATGAACTGCTGCCGACTGAGTGAC
Suflss-RKf	GTCACTCAGTCGGAAACAGTTCATTCAGGC
Suflss-RKr	GCCTGAATGAACTGTTTCCGACTGAGTGAC
Suflss-KHf	GTCACTCAGTAAACATCAGTTCATTCAGGC
Suflss-KHr	GCCTGAATGAACTGATGTTTACTGAGTGAC
Suflss-KQf	GTCACTCAGTAAACAGCAGTTCATTCAGGC
Suflss-KQr	GCCTGAATGAACTGCTGTTTACTGAGTGAC
Suflss-KKf	GTCACTCAGTAAAAAACAGTTCATTCAGGC
Suflss-KKr	GCCTGAATGAACTGTTTTTTACTGAGTGAC
Suflss-HHf	GTCACTCAGTCATCATCAGTTCATTCAGGC
Suflss-HHr	GCCTGAATGAACTGATGATGACTGAGTGAC
Sufl-noHF	CGGCGTCAGTTCATTCAGCCCCTGAAGGCCAGCGCA
Sufl-noHR	TGCGCTGGCCTTCAGGGGCTGAATGAACTGACGCCG
AmiA-nossFE	CCGGAATTCTATTACAACTCAGGCCGTATGAAAGACGAACTTTT AAAAACCAG
AmiAFATApaI-F	GCGCGGGCCCATTAAAGAGGAGAAATTAACCATGAGCACTTTT AAACCACTAAAAAC
mAmiAFATApaI-F	GCGCGGGCCCATTAAAGAGGAGAAATTAACCATGAAAGACGAA CTTTTAAAAACCAG

mAmiA-SphI-F	GCGCGCATGCGAAAAGACGAACTTTTAAAAACC
AmiAnostopBamHI-R	CGCGGATCCTCGCTTTTTCGAATGTGCTTTC
mAmiC-SphI-F	GCGCGCATGCGAGCGGTCAGCCAGGTCGTG
AmiCnostopBamHI-R	CGCGGATCCTCCCCTTCTCGCCAGCGTC
C-F94S1	GGTGTGGGCATCTATCGCCCCAG
C-F94S2	CTGGGGCGATAGATGCCCACACC
C-F94A1	GGTGTGGGCAGCGATCGCCCCAG
C-F94A2	CTGGGGCGATCGCTGCCCACACC
C-F94K1	GGTGTGGGCAAAAATCGCCCCAG
C-F94K2	CTGGGGCGATTTTTGCCCACACC
C-F94Q1	GGTGTGGGCACAGATCGCCCCAG
C-F94Q2	CTGGGGCGATCTGTGCCCACACC
C-F94R1	GGTGTGGGCACGCATCGCCCCAG
C-F94R2	CTGGGGCGATGCGTGCCCACACC
C-F94P1	GGTGTGGGCACCGATCGCCCCAG
C-F94P2	CTGGGGCGATCGGTGCCCACACC
C-F94D1	GGTGTGGGCAGATATCGCCCCAG
C-F94D2	CTGGGGCGATATCTGCCCACACC
C-F94G1	GGTGTGGGCAGGCATCGCCCCAG
C-F94G2	CTGGGGCGATGCCTGCCCACACC
C-F94C1	GGTGTGGGCATGCATCGCCCCAG
C-F94C2	CTGGGGCGATGCATGCCCACACC
B-F6Yf	GTTTGATATCGGTTATAGCGAACTGC
B-F6Yr	GCAGTTCGCTATAACCGATATCAAAC
B-L9Qf	GGTTTTAGCGAACAGCTATTGGTG
B-L9Qr	CACCAATAGCTGTTCGCTAAAACC
B-L9Pf	GGTTTTAGCGAACCGCTATTGGTG
B-L9Pr	CACCAATAGCGGTTCGCTAAAACC
B-L10Pf	GCGAACTGCCATTGGTGTTCATC
B-L10Pr	GATGAACACCAATGGCAGTTCGC
B-F13Yf	GCTATTGGTGTACATCATCGGCC
B-F13Yr	GGCCGATGATGTACACCAATAGC
B-K30If	GTGGCGGTAATTACGGTAGCGG
B-K30Ir	CCGCTACCGTAATTACCGCCAC
B-I36Nf	GTAGCGGGCTGGAATCGCGCGTTGC
B-I36Nr	GCAACGCGCGATTCCAGCCCGCTAC
tatB E8K 1	GATATCGGTTTTAGCAAACTGCTATTGG
tatB E8K 2	CCAATAGCAGTTTGCTAAAACCGATATC
C-E103A1	CGCTGTATAAGCATGCGCGTCGCCTGGTGGTGC
C-E103A2	GCACCACCAGGCGACGCGCATGCTTATACAGCG
C-P48L1	GGTATCCGCGCTGTTGATCAAGC
C-P48L2	GCTTGATCAACAGCGCGGATACC
C-M59K1	GGTTCAACGAAGATCGCCACCG
C-M59K2	CGGTGGCGATCTTCGTTGAACC

C-V145E1	CGGAAGGGGAACAGGTATCCAC
C-V145E2	GTGGATACCTGTTCCCCTTCCG
C-D211K1	CTGACGCCGCCGAAAGTCTTCTCGCAAAC
C-D211K2	GTTTGCGAGAAGACTTTCGGCGGCGTCAG
C-Q215K1	GTCTTCTCGAAAACGCTGTTG
C-Q215K2	CAACAGCGTTTTCGAGAAGAC
TatB-L9QL10P-F	GGTTTTAGCGAACAGCCATTGGTGTTCATC
TatB-L9QL10P-R	GATGAACACCAATGGCTGTTCGCTAAAACC
TatB-L10PF13Y-F	GCGAACTGCCATTGGTGTACATCATCGG
TatB-L10PF13Y-R	CCGATGATGTACACCAATGGCAGTTCGC
TatA-FB	CAGAGGAGGATCCATGGG
TatB-RS	GTATCGTCGACAGACATGC
TatCR1d	CTTGGGCTGCAGCCTTATTCTTC
TatC93R	TGCCCACACCTGATAGAG
TatCm6	CTTCCTCGAGTGATAAACCTTAAGCATG
TatC95F	ATCGCCCCAGCGCTGTAT
TatAup1-Xba I	CGCTCTAGAGAAAACCCTGCTCTACGTC
TatAup2-ClaI	GCGCATCGATAAGCTTGATATCGAAT
TatA6B7-ClaI	GCGCATCGATGATAAAGAGCAGGTGTAATCCGTGTTTGATATC GGTTTTAGC
TatCrev-KpnI	CGGGGTACCTTATTCTTCAGTTTTTTCGCTTTC
TatANcoI	GCGCCCATGGGTGGTATCAGTATTTGG
HisXba	GCGCTCTAGATTAGTGATGGTGATGGTG
STIPE-ISH	GCGGATACGAATCAGGAACAG
pT7.5R	CGCTGAGATAGGTGCC.
p101C*BCflag_F	GAAAGCGAAAAAACTGAAGAAGACTACAAGGACGATGACAAGT AAGGCTGCAGGCATGCAAG
p101C*BCflag_R	CTTGCATGCCTGCAGCCTTACTTGTCATCGTCCTTGTAGTCTTC TTCAGTTTTTTCGCTTTC

Table S5. Oligonucleotides used in this study

Supplementary References

1. Casadaban MJ, Cohen SN (1979) Lactose genes fused to exogenous promoters in one step using a Mu-lac bacteriophage: *in vivo* probe for transcriptional control sequences. *Proc Natl Acad Sci USA* 76(9):4530-4533.

2. Wexler M*, et al.* (2000) TatD is a cytoplasmic protein with DNase activity. No requirement for TatD family proteins in sec-independent protein export. *J Biol Chem* 275(22):16717-16722.

3. Lee PA*, et al.* (2006) Cysteine-scanning mutagenesis and disulfide mapping studies of the conserved domain of the twin-arginine translocase TatB component. *J Biol Chem* 281(45):34072-34085.

4. Alcock F*, et al.* (2013) Live cell imaging shows reversible assembly of the TatA component of the twin-arginine protein transport system. *Proc Natl Acad Sci USA* 110(38):E3650-3659.

5. Keller R, de Keyzer J, Driessen AJ, Palmer T (2012) Co-operation between different targeting pathways during integration of a membrane protein. *Journal Cell Biol* 199(2):303-315.

6. Datsenko KA, Wanner BL (2000) One-step inactivation of chromosomal genes in *Escherichia coli* K-12 using PCR products. *Proc Natl Acad Sci USA* 97(12):6640-6645.

7. Kneuper H*, et al.* (2012) Molecular dissection of TatC defines critical regions essential for protein transport and a TatB-TatC contact site. *Mol Microbiol* 85(5):945-961.

8. Hashimoto-Gotoh T*, et al.* (2000) A set of temperature sensitive-replication/-segregation and temperature resistant plasmid vectors with different copy numbers and in an isogenic background (chloramphenicol, kanamycin, *lacZ*, *repA*, *par*, *polA*). *Gene* 241(1):185-191.

9. Cléon F*, et al.* (2015) The TatC component of the twin-arginine protein translocase functions as an obligate oligomer. *Mol Microbiol* 98(1):111-129.

10. Maldonado B*, et al.* (2011) Characterisation of the membrane-extrinsic domain of the TatB component of the twin arginine protein translocase. *FEBS Lett* 585(3):478-484.

11. Jack RL*, et al.* (2004) Coordinating assembly and export of complex bacterial proteins. *EMBO J* 23(20):3962-3972.

12. Ize B, Stanley NR, Buchanan G, Palmer T (2003) Role of the *Escherichia coli* Tat pathway in outer membrane integrity. *Mol Microbiol* 48(5):1183-1193.

13. Tarry MJ*, et al.* (2009) Structural analysis of substrate binding by the TatBC component of the twin-arginine protein transport system. *Proc Natl Acad Sci USA* 106(32):13284-13289.

14. Hamilton CM, Aldea M, Washburn BK, Babitzke P, Kushner SR (1989) New method for generating deletions and gene replacements in *Escherichia coli*. *J Bacteriol* 171(9):4617-4622.

15. Guzman LM, Belin D, Carson MJ, Beckwith J (1995) Tight regulation, modulation, and high-level expression by vectors containing the arabinose P_{BAD} promoter. *J Bacteriol* 177(14):4121-4130.

Supplementary Figure Legends

Figure S1. Substitutions of the twin arginines in the AmiA signal peptide prevent growth in the presence of SDS. Strain MCDSSAC Δ*tatABC* producing wild type *tatABC* from plasmid pTAT1d and either wild type ('RR') or signal peptide point-substituted AmiA, as indicated, from pSUAmiA. The strain and plasmid combinations were cultured overnight in LB medium supplemented with chloramphenicol and ampicillin (for plasmid selection), after which they were streaked onto LB agar containing the same antibiotics, with and without the addition of 2% SDS and incubated for 16 hr at 37°C.

Figure S2. TatB variants are able to restore Tat transport to a range of defective twin arginine substitutions in the AmiA signal sequence. Growth of MCDSSAC Δ*tatABC* coproducing the indicated TatB variants (with wild type *tatA* and *tatC*) from pTAT101, or the empty plasmid pTH19kr (indicated by '*Δtat*') alongside signal peptide variants of AmiA, on LB agar supplemented with chloramphenicol and kanamycin, with and without the addition of 2% SDS as indicated. An 8μl aliquot of each strain/plasmid combination following aerobic growth to an OD_{600} of 1.0 was spotted and incubated for 16 hr at 37°C. A. Individual signal peptide substitutions of AmiA (indicated to the left of each panel) were tested against the TatB suppressors F6Y, L9P, L9Q, L10P, F13Y, K30I and I36N. B. The TatB E8K suppressor was tested for the ability to suppress the indicated AmiA signal peptide substitutions.

Figure S3. TatB variants are able to restore Tat transport to a range of defective twin arginine substitutions in the SufI signal sequence. Growth of MCDSSAC Δ*tatABC* coproducing the indicated TatB variants (with wild type *tatA* and *tatC*) from pTAT101, or the empty plasmid pTH19kr (indicated by '*Δtat*') alongside signal peptide variants of SufI fused to the AmiA mature domain, on LB agar supplemented with chloramphenicol and kanamycin, with and without the addition of 2% SDS as indicated. An 8μl aliquot of each strain/plasmid combination following aerobic growth to an OD_{600} of 1.0 was spotted and incubated for 16 hr at 37°C. A. Individual signal peptide substitutions of AmiA (indicated to the left of each panel) were tested against the TatB suppressors F6Y, L9P, L9Q, L10P, F13Y, K30I and I36N. B. The

TatB E8K suppressor was tested for the ability to suppress the indicated AmiA signal peptide substitutions

Figure S4. A subset of amino acid substitutions at TatCF94 abolish Tat activity when produced at medium and low copy number. A and C. Growth of DADE coproducing either wild type TatABC (Tat^+), wild type TatAB alongside F94-substituted TatC or the cognate empty plasmid (Tat^-) on LB agar containing 2% SDS. A single colony of each strain/plasmid combination was resuspended in 30μl of PBS and an 8μl aliquot was spotted onto LB agar supplemented with appropriate antibiotics, along with 2% SDS as indicated. Plates were incubated for 16 hr at 37°C. B and D. Detection of TatC protein present in membrane fractions of the same strain and plasmid combinations as in A. and C., respectively, by Western immunoblot with anti-TatC antiserum. A total of 5μg membranes was loaded per lane for TatC produced from pTAT1d (B) and 20μg per lane for membranes produced from strains harboring pTAT101 derivatives (D).

Figure S5. TatB variants cannot supress TatC inactivating substitutions outside of the signal peptide binding site. Growth of DADE (Δ*tatABCD*, Δ*tatE*) coproducing wild type TatA alongside and the indicated substitution in TatB alongside either of TatC P48L, TatC M59K, TatC V145E, TatC D211K or TatC Q215K as indicated, from plasmid pTAT101 on LB agar or LB agar containing 2% SDS. A single colony of each strain/plasmid combination was resuspended in 30μl of PBS and an 8μl aliquot was spotted onto LB agar supplemented with appropriate antibiotics, along with 2% SDS as indicated, and incubated for 16 hr at 37°C.

Figure S6. The suppressive effect of the TatB variants is not additive and mature AmiC is not exported in the presence of the TatB F13Y suppressor. A. Growth of DADE coproducing either wild type TatABC (Tat^+), wild type TatAB alongside F94-substituted TatC or the cognate empty plasmid (Tat^-) on LB agar or LB agar containing 2% SDS. B. Growth of MCDSSAC Δ*tatABC* coproducing the indicated TatB variants (with wild type *tatA* and *tatC*) from pTAT101, or the empty plasmid pTH19kr (indicated by '*Δtat*') alongside the RN or KK

signal peptide variants of SufI fused to the AmiA mature domain, as indicated, on LB agar with or without the addition of 2% SDS. C. Strain MC4100 Δ*ami*A Δ*amiC* Δ*tatABC* coproducing either wild-type TatB or TatB F13Y (with wild type *tatA* and *tatC*) from pTAT101 and the AmiA or AmiC mature domains (from pQE70-mAmiA or pQE70-mAmiC, respectively) on LB agar or LB agar containing 2% SDS. In each case a single colony of each strain/plasmid combination was resuspended in 30μl of PBS and an 8μl aliquot was spotted onto LB agar supplemented with appropriate antibiotics, along with 2% SDS where indicated. Plates were incubated for 16 hr at 37°C.

Figure S7. The TatB suppressors support export of his-tagged SufI with its native signal peptide. A. and B. *E. coli* strain DADE producing wild type TatA and TatC and the indicated TatB variants alongside wild-type SufI-his or the indicated signal-peptide variants were fractionated into whole cell (upper panels) and periplasm (lower panels) fractions, then analysed by Western blot with anti-6X His tag® or anti-RNA polymerase β subunit antibodies (cytoplasmic control protein). wc – whole cell.

Figure S8. TatBC and SufIss-GFP-His twin-arginine variants are detectable in whole cell samples. A. and B. Cells producing SufIss-GFP-His with the wild type (RR) or twin-arginine substituted SufI signal peptide, as indicated, alongside TatC and either wild type TatB or the E8K, F13Y or I36N substituted variants, or C. and D. Cells producing SufIss-GFP-His with the wild type SufI signal peptide along with either wild type TatBC, the TatC F94Q allele along with either wild type TatB or the L9Q, L10P, F13Y or I36N substituted variants, or the TatC E103K allele along with either wild type TatB or the L9Q, L10P, F13Y or I36N substituted variants, as indicated were harvested and resuspended in PBS. A. and C. The fluorescence intensity and OD_{600} of the samples were measured using a plate reader and the Fluorescence/OD_{600} plotted for each sample. B. and D. 20 µl of each cell suspension was taken, all samples were normalized to the same OD_{600} and then analysed by SDS-PAGE followed by western blot using a TatB-TatC mixed antibody.

Figure S9. TatBC complexes containing the TatB F13Y suppressor do not co-purify with signal peptide variants of AmiA. C-terminally his-tagged wild type AmiA, twin-arginine substituted AmiA or signal sequence-less AmiA, as indicated was co-produced alongside wild type TatBC or TatBF13Y/TatC and purified using nickel beads from digitonin–treated cell extracts. Aliquots of the load and elution fractions were subject to SDS-PAGE followed by Western blot using either anti-His, anti-TatB and TatC antibodies.

Figure S10. TatB variants are extracted from the membrane with digitonin. Membrane suspensions (containing equivalent amounts of total protein) from strain DADE coproducing either wild type TatABC or wild type TatA and TatC alongside the indicated amino acid variant of TatB were solubilized by addition of 2% digitonin and incubation on ice for 30 min. Samples total membranes and digitonin solubilized material (each containing 10μg protein) were analysed by SDS-PAGE followed by western blotting with anti-TatA, anti-TatB or anti-TatC antibodies as indicated.

Figure S11. Constitutive oligomerisation of TatA is not promoted by the TatB L9Q, L10P or I36N substitutions. Fluorescence images of TatA-YFP in representative cells of A. strains AyBCE or AyBC_{F94Q}E (encoding chromosomal TatC F94Q) in the presence (pAmiA) or absence of plasmid-encoded wild type AmiA, as indicated (reproduced from Fig 5A). B. strains AyB_{L9Q}CE (encoding chromosomal TatB L9Q), AyB_{L10P}CE (encoding chromosomal TatB L10P) and AyB_{I36N}CE (encoding chromosomal TatB I36N) or the same strains additionally harboring the chromosomally-encoded TatC F94Q substitution. Scale bar: 1 μm. Note that the pictures in panel A are identical to those in Fig 5A and were included here to provide a direct comparison with panel B.

LB LB + 2% SDS

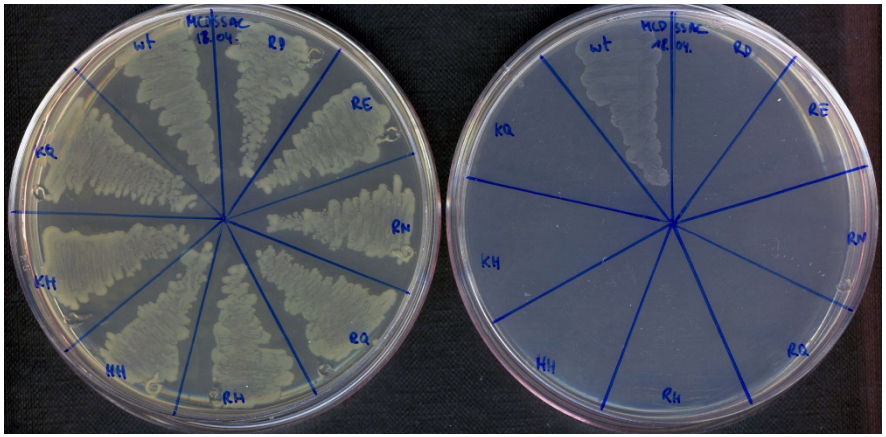

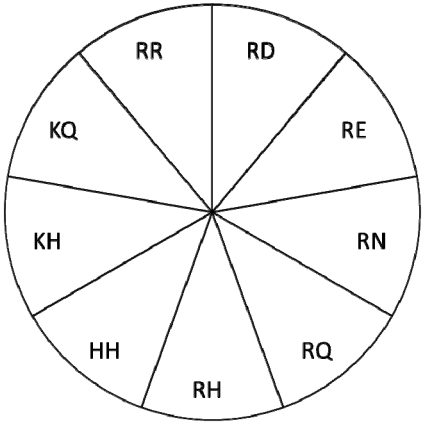

Fig S1

A

WT TatB	Δ*tat*	TatB F6Y
TatB L9P	TatB L9Q	TatB L10P
TatB F13Y	TatB K30I	TatB I36N

WT TatB	Δ*tat*	TatB F6Y
TatB L9P	TatB L9Q	TatB L10P
TatB F13Y	TatB K30I	TatB I36N

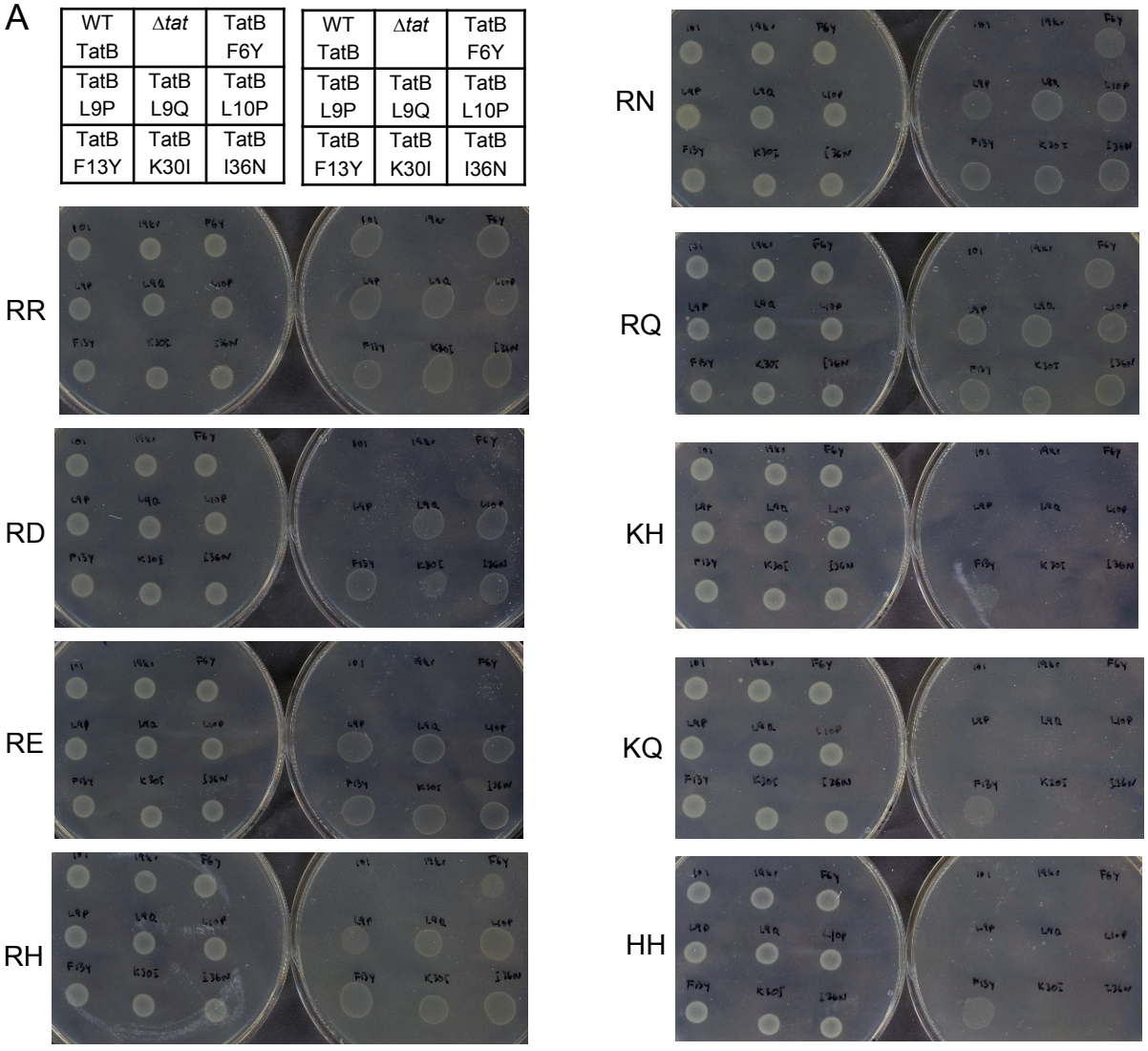

B

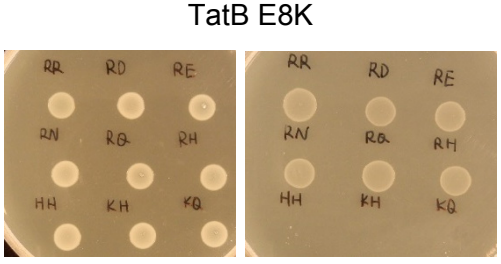

AmiA RR	AmiA RD	AmiA RE
AmiA RN	AmiA RQ	AmiA RH
AmiA HH	AmiA KH	AmiA KQ

Fig S2

A

WT TatB	Δ*tat*	TatB F6Y
TatB L9P	TatB L9Q	TatB L10P
TatB F13Y	TatB K30I	TatB I36N

WT TatB	Δ*tat*	TatB F6Y
TatB L9P	TatB L9Q	TatB L10P
TatB F13Y	TatB K30I	TatB I36N

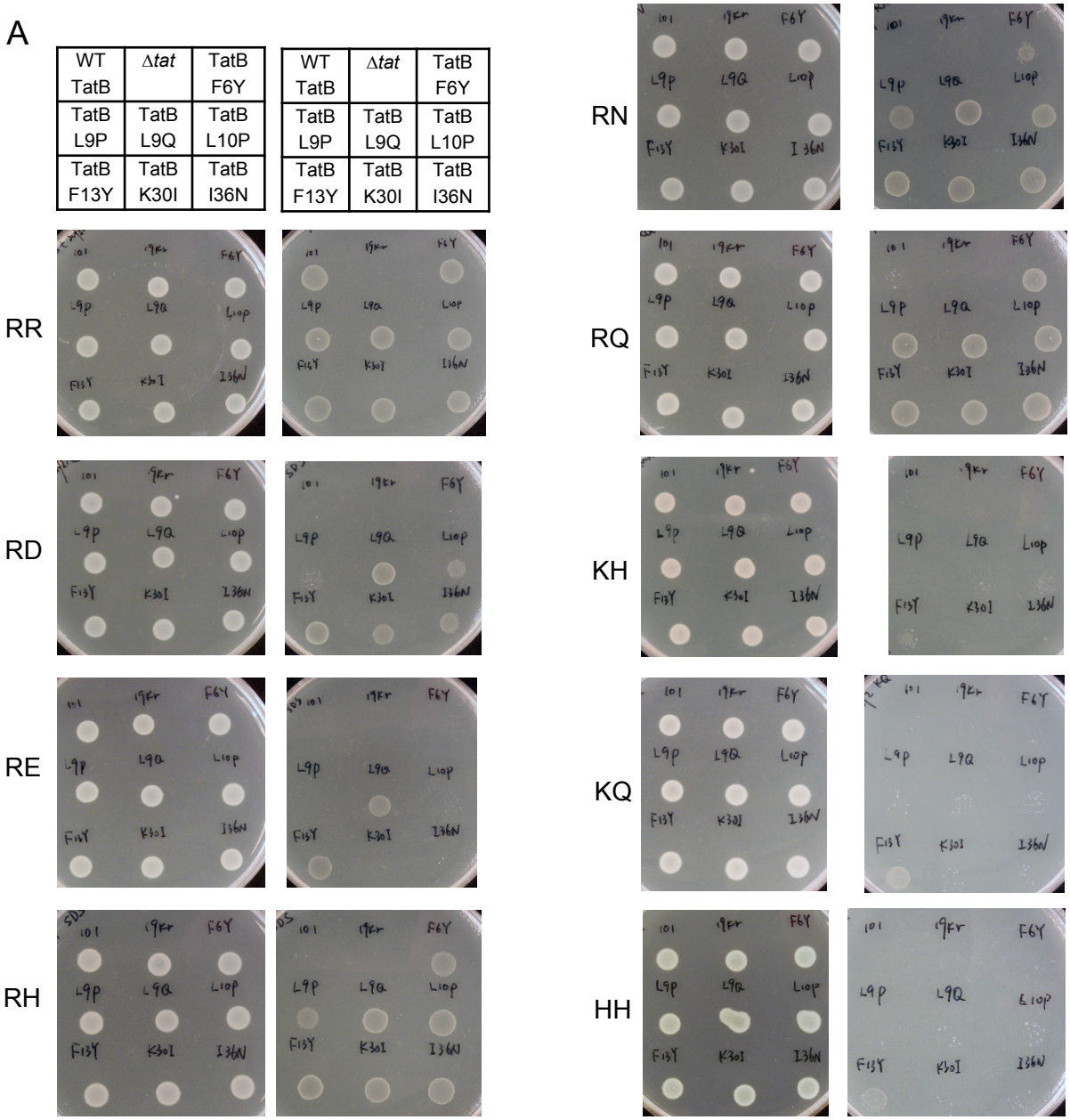

B

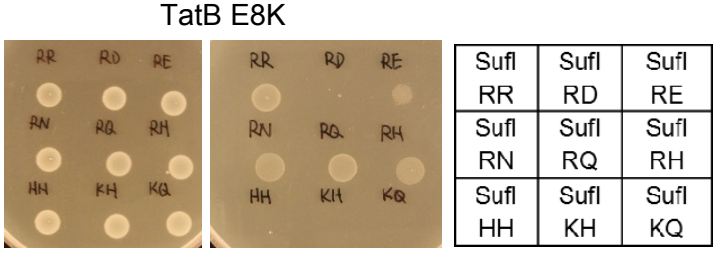

SufI RR	SufI RD	SufI RE
SufI RN	SufI RQ	SufI RH
SufI HH	SufI KH	SufI KQ

Fig S3

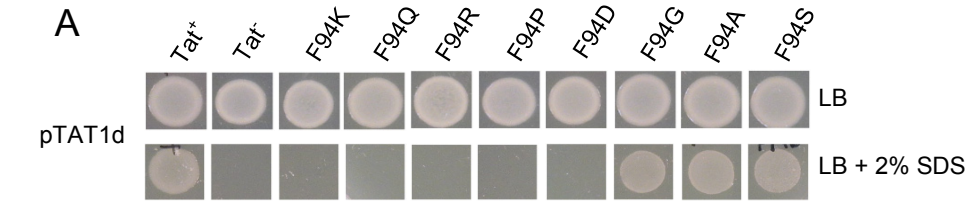
A
Tat+
Tat-
F94K
F94Q
F94R
F94P
F94D
F94G
F94A
F94S
pTAT1d
LB
LB + 2% SDS

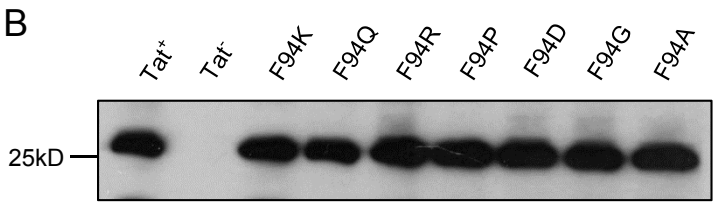
B
Tat+
Tat-
F94K
F94Q
F94R
F94P
F94D
F94G
F94A
25kD

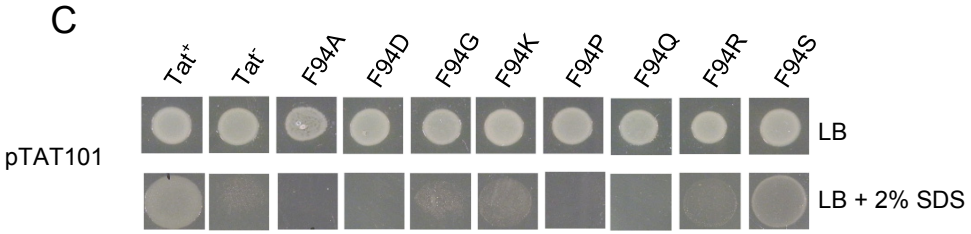
C
Tat+
Tat-
F94A
F94D
F94G
F94K
F94P
F94Q
F94R
F94S
pTAT101
LB
LB + 2% SDS

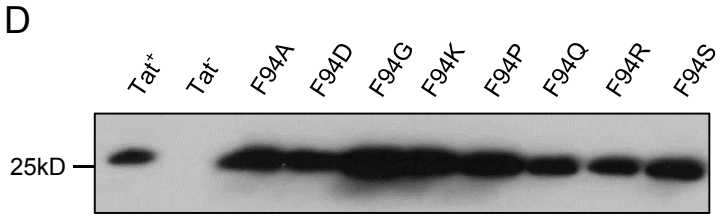
D
Tat+
Tat-
F94A
F94D
F94G
F94K
F94P
F94Q
F94R
F94S
25kD

Fig S4

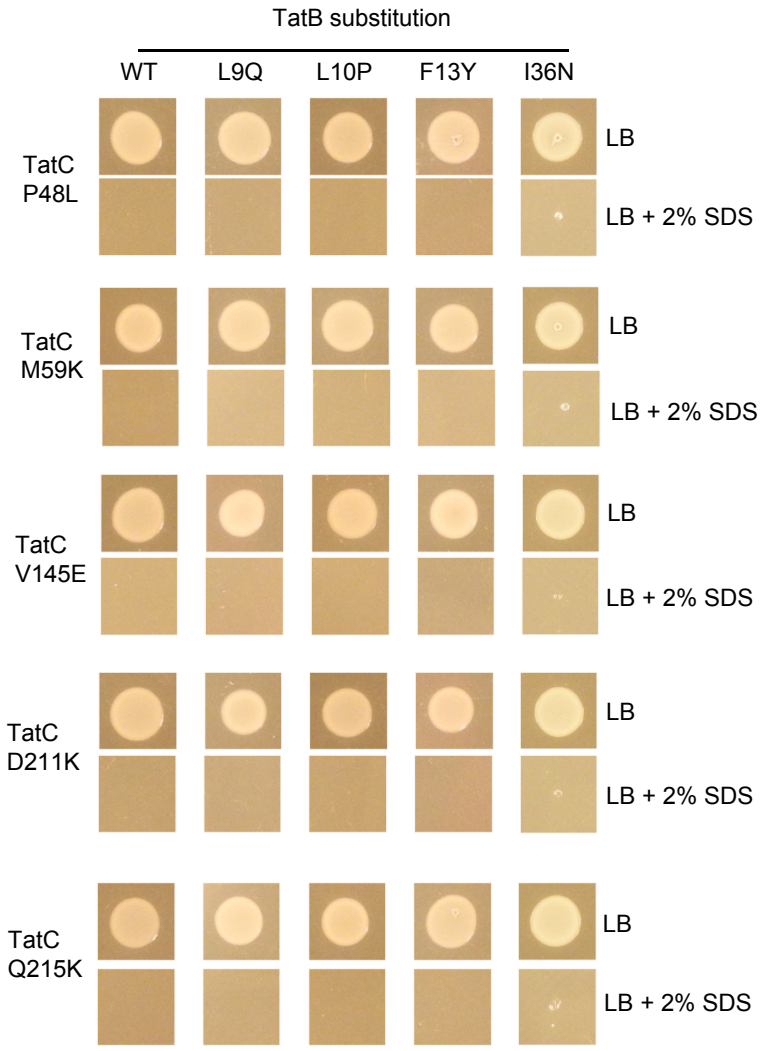
TatB substitution
WT
L9Q
L10P
F13Y
I36N
TatC P48L
TatC M59K
TatC V145E
TatC D211K
TatC Q215K
LB
LB + 2% SDS

Fig S5

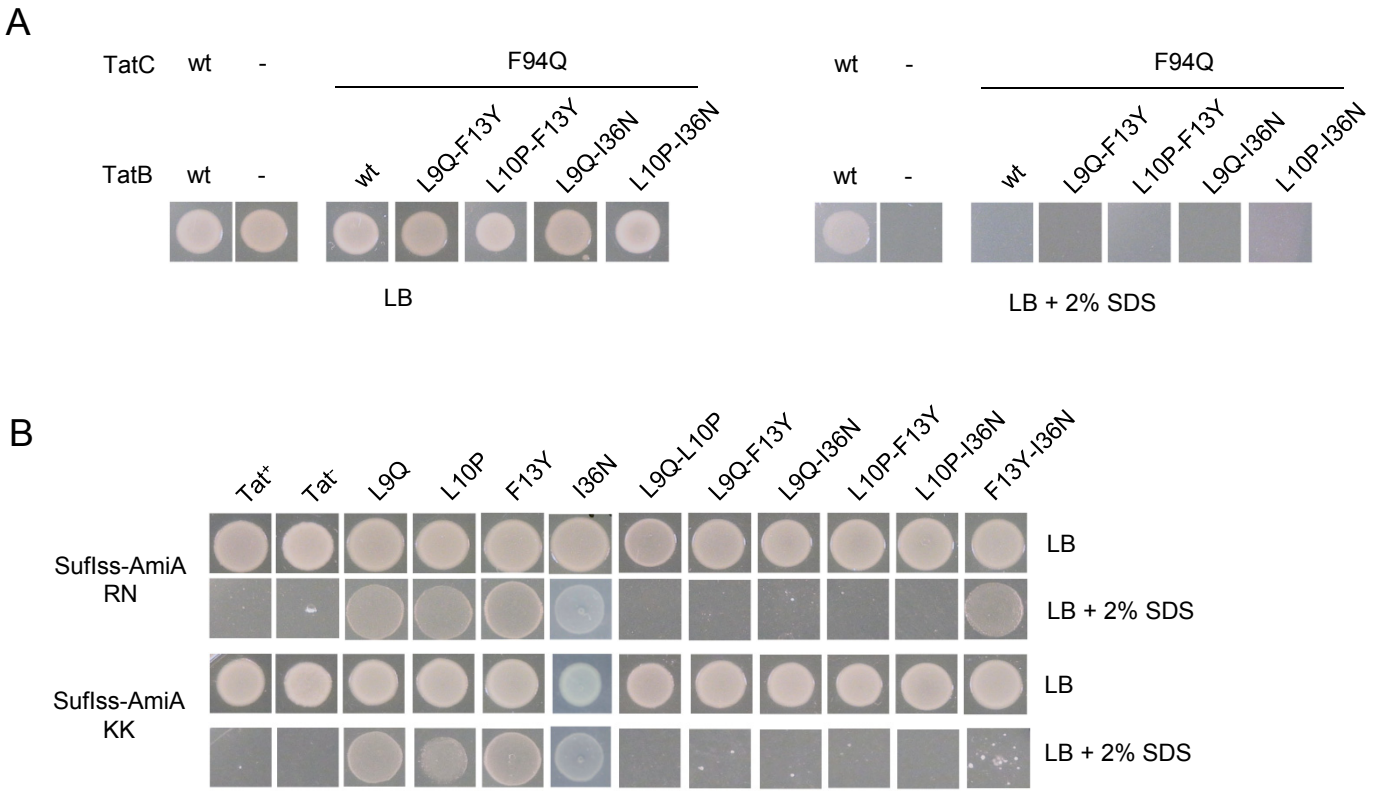
A
TatC
wt
-
F94Q
TatB
wt
-
wt
L9Q-F13Y
L10P-F13Y
L9Q-I36N
L10P-I36N
LB
LB + 2% SDS
B
Tat+
Tat-
L9Q
L10P
F13Y
I36N
L9Q-L10P
L9Q-F13Y
L9Q-I36N
L10P-F13Y
L10P-I36N
F13Y-I36N
SufIss-AmiA RN
SufIss-AmiA KK
LB
LB + 2% SDS
C
mAmiA
mAmiC
TatB
wt
F13Y
LB
LB + 2% SDS

Fig S6

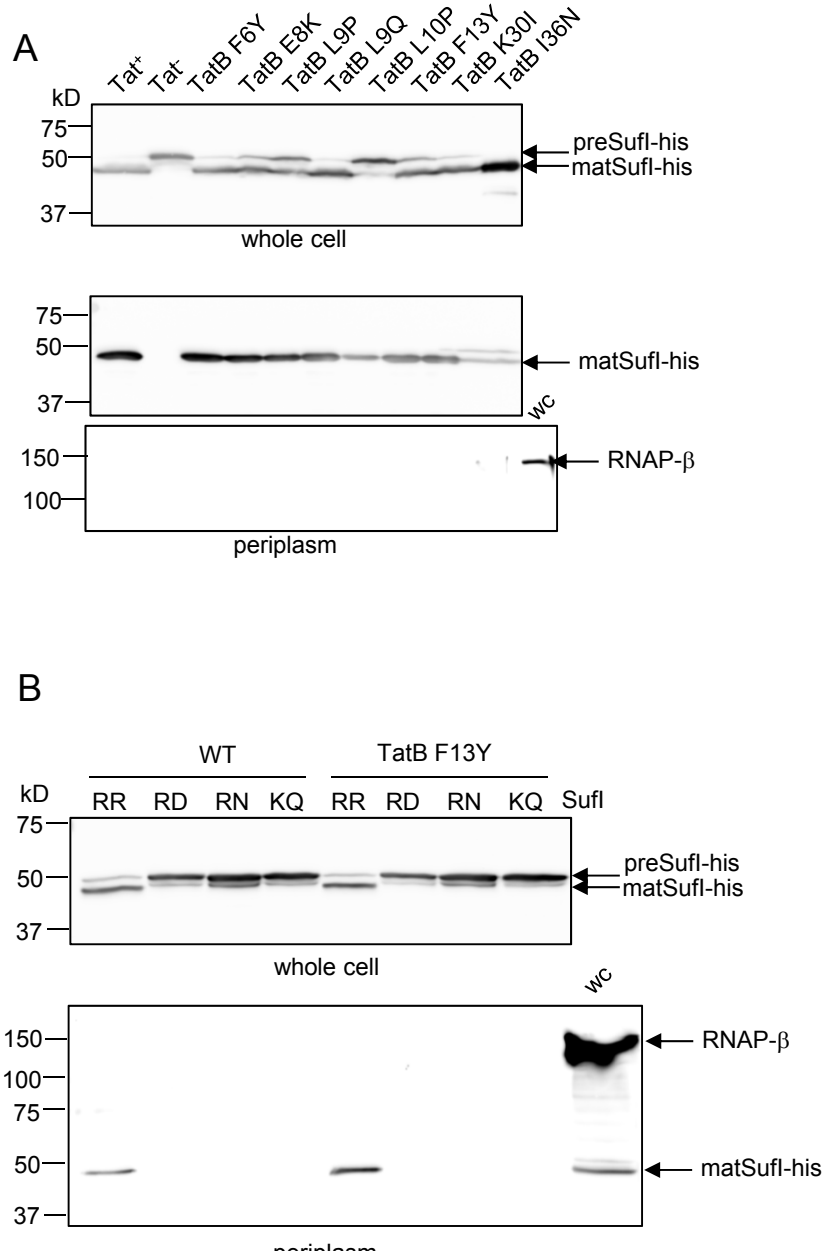
A
Tat+
Tat-
TatB F6Y
TatB E8K
TatB L9P
TatB L9Q
TatB L10P
TatB F13Y
TatB K30I
TatB I36N
kD
75
50
37
preSufI-his
matSufI-his
whole cell
75
50
37
matSufI-his
WC
150
100
RNAP-β
periplasm
B
WT
TatB F13Y
kD
RR
RD
RN
KQ
RR
RD
RN
KQ
SufI
75
50
37
preSufI-his
matSufI-his
whole cell
WC
150
100
75
50
37
RNAP-β
matSufI-his
periplasm

Fig S7

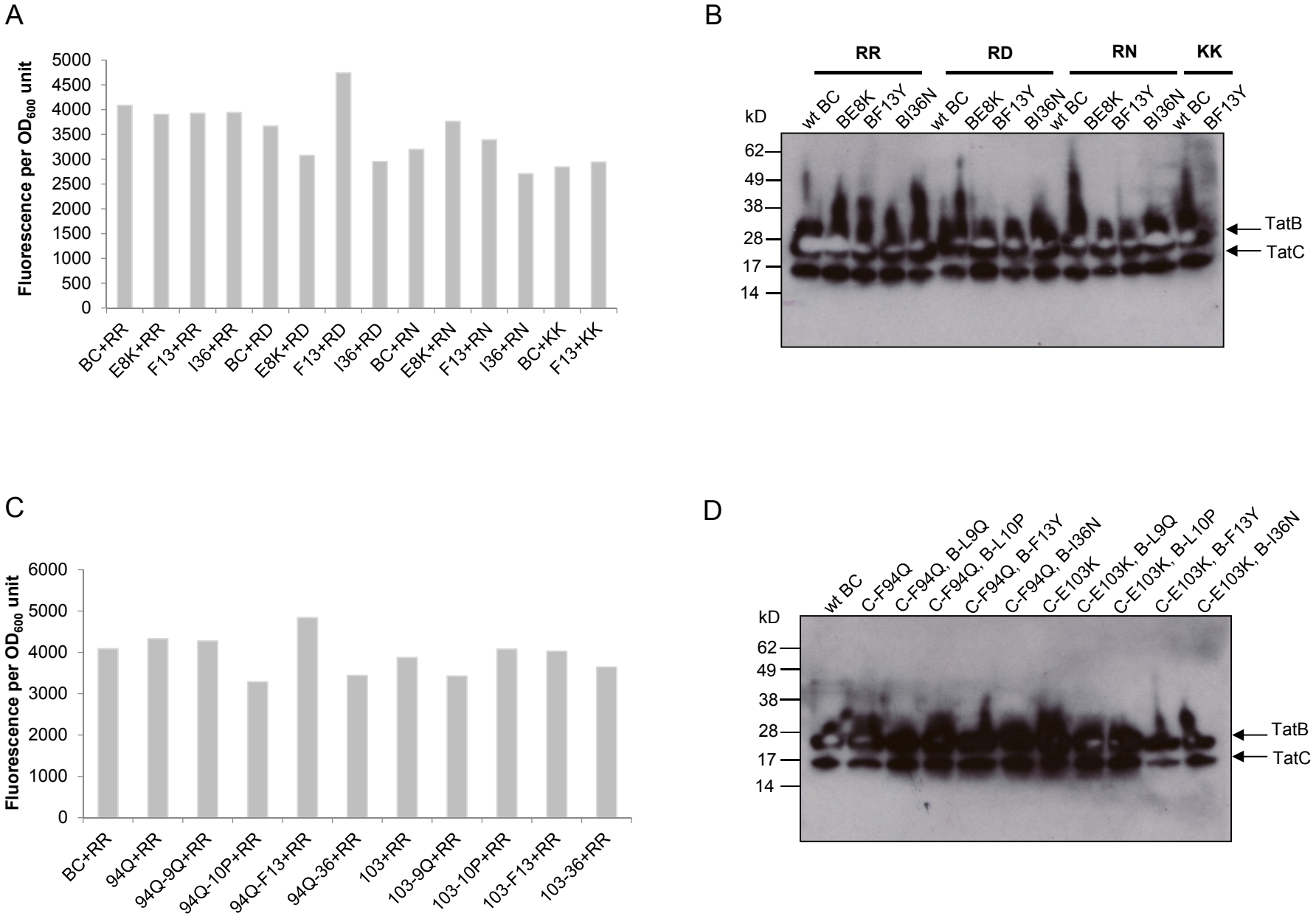
A
Fluorescence per OD600 unit
5000
4500
4000
3500
3000
2500
2000
1500
1000
500
0
BC+RR
E8K+RR
F13+RR
I36+RR
BC+RD
E8K+RD
F13+RD
I36+RD
BC+RN
E8K+RN
F13+RN
I36+RN
BC+KK
F13+KK
B
RR
RD
RN
KK
kD
wt BC
BE8K
BF13Y
BI36N
wt BC
BE8K
BF13Y
BI36N
wt BC
BE8K
BF13Y
BI36N
wt BC
BF13Y
62
49
38
28
17
14
TatB
TatC
C
Fluorescence per OD600 unit
6000
5000
4000
3000
2000
1000
0
BC+RR
94Q+RR
94Q-9Q+RR
94Q-10P+RR
94Q-F13+RR
94Q-36+RR
103+RR
103-9Q+RR
103-10P+RR
103-F13+RR
103-36+RR
D
wt BC
C-F94Q
C-F94Q, B-L9Q
C-F94Q, B-L10P
C-F94Q, B-F13Y
C-F94Q, B-I36N
C-E103K
C-E103K, B-L9Q
C-E103K, B-L10P
C-E103K, B-F13Y
C-E103K, B-I36N
kD
62
49
38
28
17
14
TatB
TatC

Fig S8

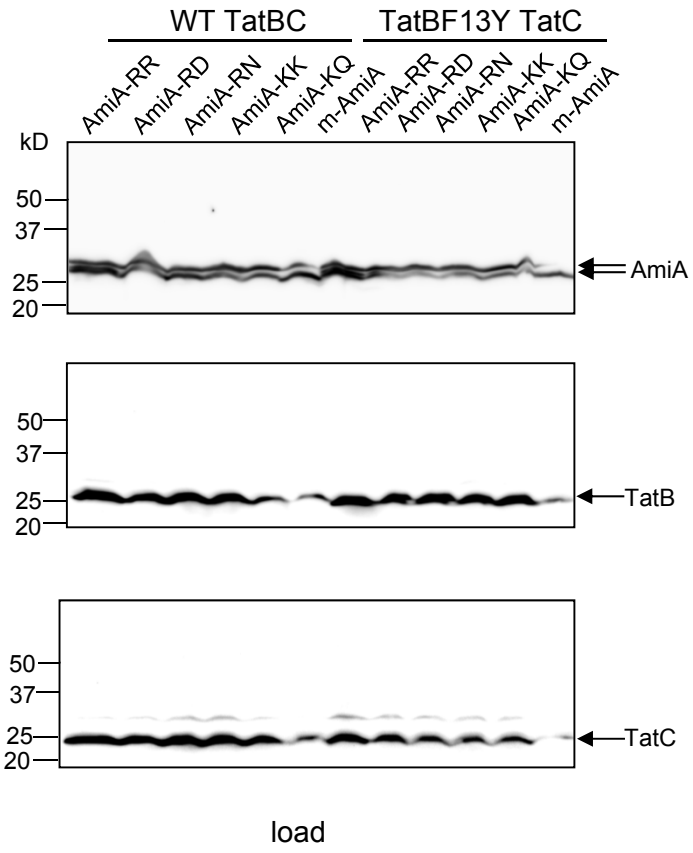
WT TatBC
TatBF13Y TatC
AmiA-RR
AmiA-RD
AmiA-RN
AmiA-KK
AmiA-KQ
m-AmiA
kD
50
37
25
20
AmiA
TatB
TatC
load

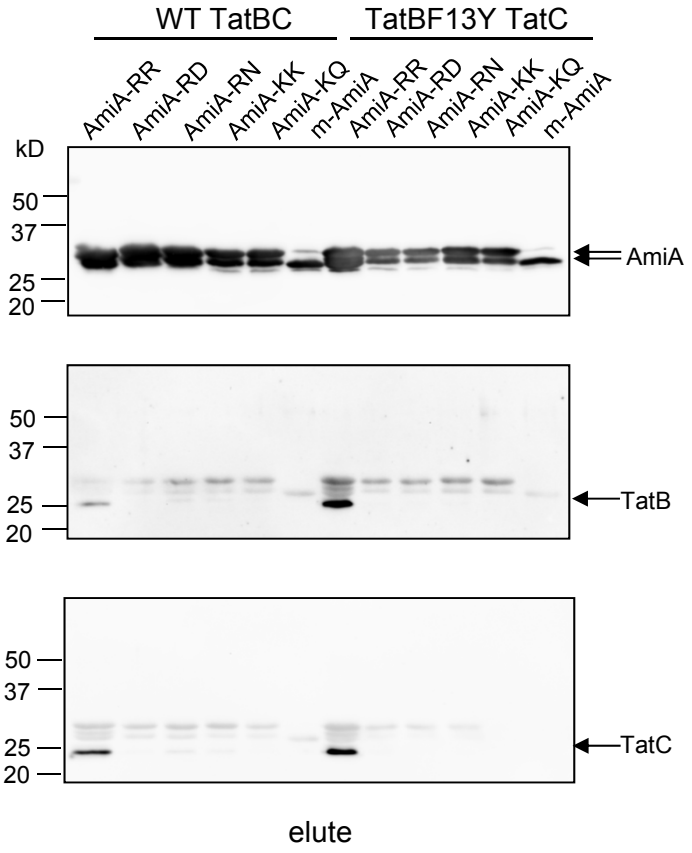
WT TatBC
TatBF13Y TatC
AmiA-RR
AmiA-RD
AmiA-RN
AmiA-KK
AmiA-KQ
m-AmiA
kD
50
37
25
20
AmiA
TatB
TatC
elute

Fig S9

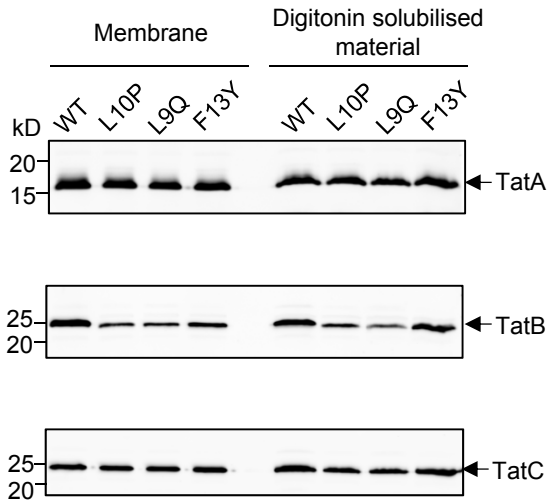
Membrane
Digitonin solubilised material
kD
WT
L10P
L9Q
F13Y
WT
L10P
L9Q
F13Y
20
15
TatA
25
20
TatB
25
20
TatC

Fig S10

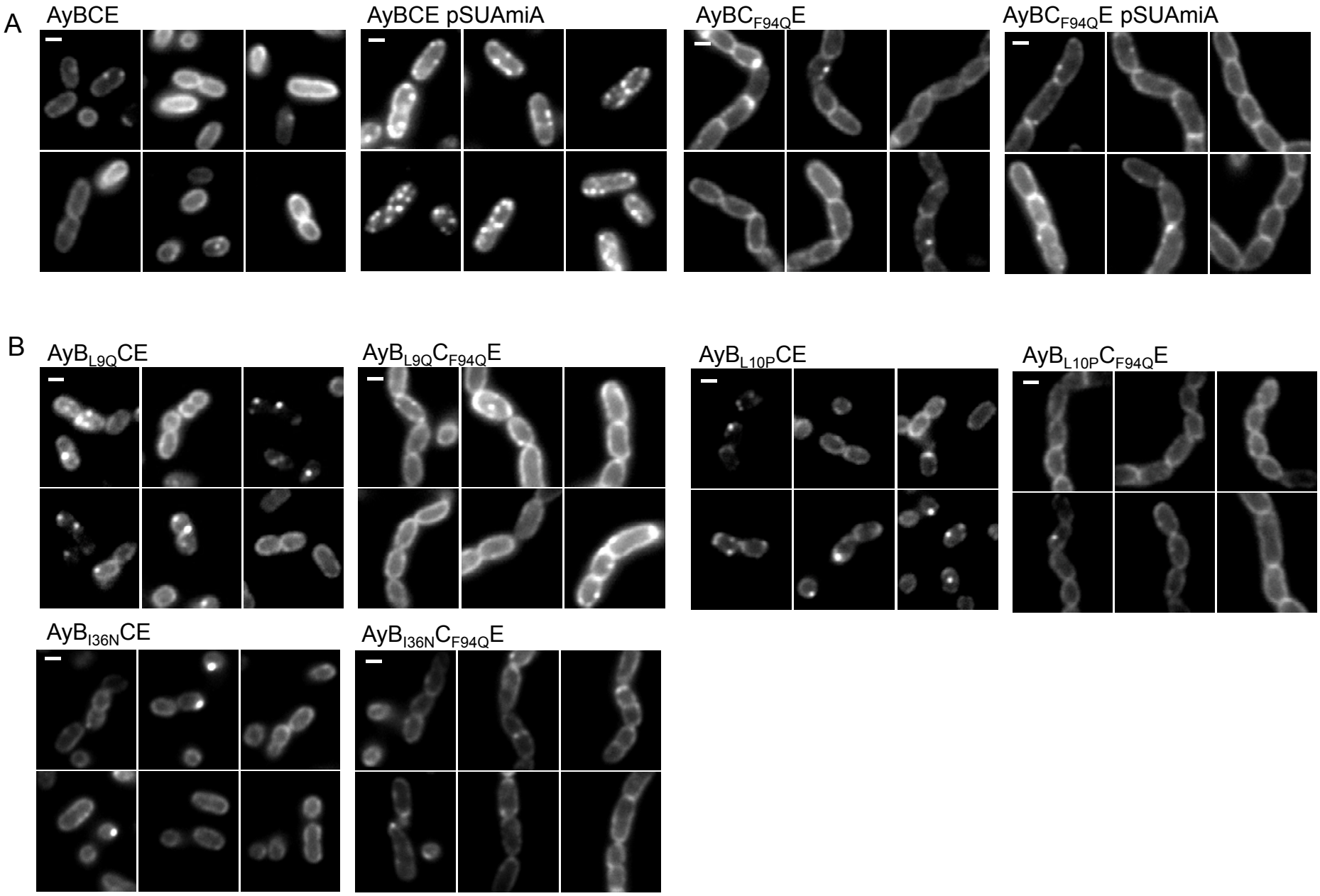
A
AyBCE
AyBCE pSUAmiA
AyBC$_{F94Q}$E
AyBC$_{F94Q}$E pSUAmiA
B
AyB$_{L9Q}$CE
AyB$_{L9Q}$C$_{F94Q}$E
AyB$_{L10P}$CE
AyB$_{L10P}$C$_{F94Q}$E
AyB$_{I36N}$CE
AyB$_{I36N}$C$_{F94Q}$E

Fig S11